The Subsynoptic Scale Model and Investigations of the Value of Satellite Sounding Data in Numerical Weather Prediction

A REPORT

from the space science and engineering center
the university of wisconsin-madison
madison, wisconsin

The Subsynoptic Scale Model and Investigations of the Value of Satellite Sounding Data in Numerical Weather Prediction

Graham Mills
Australian Numerical Meteorological Research Centre

George R. Diak, Ph.D
University of Wisconsin-Madison
Space Science and Engineering Center
1225 West Dayton Street
Madison, Wisconsin 53706

Christopher Hayden, Ph.D
NOAA/NESDIS Development Laboratory
1225 West Dayton Street
Madison, Wisconsin 53706

May 1983

TABLE OF CONTENTS

ACKNOWLEDGMENTS

The work which is described in this report represents the efforts of many scientists in the National Environmental Satellite, Data, and Information Service Development Laboratory (NESDIS/DL) of the National Oceanic and Atmospheric Administration (NOAA), the University of Wisconsin-Madison, the Space Science and Engineering Center (SSEC), and the Australian Numerical Meteorological Research Centre (ANMRC). Much of the discussion of model results is capasulized from two previous reports, Mills et al. (1980) and Mills and Hayden (1983).

ABSTRACT

This report describes progress to date in an effort to develop and test a subsynoptic scale model, a tool designed to help assess the value of satellite temperature and moisture soundings in numerical weather prediction. Analysis and forecast model characteristics are outlined. Results of several forecasts are evaluated and an experiment using TIROS-N satellite soundings to update the forecast model for the Red River tornado episode of April 10, 1979 is described.

Finally, the experiments to be completed in the next year are outlined.

1. INTRODUCTION

The National Environmental Satellite Data, and Information Service Development Laboratory (NESDIS/DL) has for over four years been developing techniques for producing sets of atmospheric temperature and moisture profiles with a high spatial resolution using the Man-computer Interactive Data Access System (McIDAS). A prime indicator of the value of these new data is their impact in numerical weather prediction.

This report summarizes progress to data in an ongoing colaborative effort between NESDIS/DL, the Space Science and Engineering Center (SSEC) at the University of Wisconsin-Madison, and the Australian Numerical Meteorological Research Centre (ANMRC) in an experiment designed to impliment a Subsynoptic Scale Model (SSM) and test the value of high-resolution satellite retrievals in numerical prediction.

2. BACKGROUND--THE PROBLEM

Two requirements for accurate short term numerical weather forecasting are complete and accurate initial data and a forecast model with commensurate numerical resolution. In the latter case, it has been shown in several studies (Miyakoda and Rosati, 1977; Shuman, 1978; Leslie, 1981) that synoptic scale numerical weather predictions increase in accuracy when the grid spacing is reduced. The continuity of this forecast improvement as it carries over to mesoscale models (resolution < 100 km) is less well understood. In principal at least it has been documented (Anthes and Warner, 1978; Bleck, 1977) that in conditions where local forcing (topography, land-sea effect) play an important role in atmospheric evolution, the details of the initial state are not as important as correct physical modelling of the situation. Whether or not the increased detail is, in fact, a forecast improvement is difficult to document because of

the scarcity of high-resolution verifying data. In these cases, however, the increased detail is qualitatively reasonable.

Improvement in forecast skill resulting from improved initial data has been more difficult to establish. Most recently, with improved assimilation techniques and better data, satellite reports have been found to positively impact hemispheric forecasts (Halem et al., 1982). Impact in the southern hemisphere has been easier to demonstrate (Kelly et al., 1978) undoubtedly due to the enormous difference in the ground-based upper air observing networks north and south of the equator. Indications are that when the conventional network is inadequate to resolve the scale being forecast (south of the equator this is the synoptic scale) satellite retrievals positively impact numerical prognosis. The conventional network over the U.S. well-resolves the synoptic scale, but the network is inadequate to resolve important mesoscale features such as sharp moisture gradients associated with severe weather outbreaks.

Recently, satellite derived meteorological data with mesoscale resolution have become routinely available using manually interactive techniques on the McIDAS computer at the University of Wisconsin-Madison. Two data sources are cloud vector winds derived from geostationary satellite data (Wilson and Houghton, 1979) and vertical temperature and moisture profiles derived from the TIROS-N and VAS instruments. Work has been done by Lee and Houghton (1981) assimilating vector wind data into a mesoscale numerical model. Tarbell et al. (1981) have shown that increased detail in temperature and moisture forecasting significantly improves model forecasts of rainfall, particularly in early stages of model integration. If mass and wind data were to be available with a resolution comparable to the resolution of mesoscale models, numerical forecasts may show improved accuracy.

3. SSM PROGRAM HISTORY

The cooperative program between the ANMRC, SSEC and NESDIS/DL began in 1976 while NESDIS/DL Chief, W. L. Smith, was a visiting scientist to the ANMRC. During his visit, the ANMRC successfully demonstrated the impact of NIMBUS-6 soundings on Australian region forecasts (Kelly et al., 1978). In that study an operational primitive-equation model (McGregor et al., 1978) with 250 km horizontal resolution used satellite soundings with 150 km horizontal resolution.

At that time, in view of the anticipated characteristics of forthcoming sounding data, the development of a limited-area analysis-forecast system of approximately 60 km was considered essential. The ANMRC had already developed an extensively tested limited-area objective analysis and forecast model over the Australian region, in both operational and research models, at resolutions of 250 and 125 km respectively. Thus, initially, it was a straightforward task to adapt the 125 km version to a still higher resolution over the North American region. The first work towards this goal was done on the Australian CDC-CYBER-76 computer with a four-level model version.

During 1979-1980 G. Kelly from ANMRC worked at the University of Wisconsin-Madison with NESDIS/DL and SSEC scientists to impliment the ANMRC model at ten-level vertical resolution on the CRAY-1 computer at the National Center for Atmospheric Research (NCAR). Beginning in January 1981, G. Mills joined the SSEC-NESDIS/DL group as visiting scientist for the year and incorporated numerous improvements in the system for analyzing the satellite data. Most recently, the analysis-forecast system has been converted to the new IBM 4341 computer at SSEC. Beginning in

February 1983, J. LeMarshall from the ANMRC began a year stay at SSEC. Part of his responsibility will be to convert and test a limited-area normal mode initialization scheme developed at ANMRC to the UW-Madison system.

4. SUBSYNOPTIC SCALE MODEL DESCRIPTION

4.1 Analysis system

The area analyzed by the CRAY and IBM 4341 SSM analysis model versions are shown in Figure 1. A Lambert conformal projection is used with a grid spacing of about 67 km at standard latitudes.

The pressure levels used in the analysis are 1000, 850, 700, 500, 400, 300, 250, 150 and 100 mb. At each of these levels geopotential height, temperature, dewpoint depression (levels from 1000 to 500 mb) wind, and stream function are either analysed or diagnosed. Mean sea level pressure is analyzed and used to provide a reference level for the remainder of the analysis.

4.2 Analysis Methodology

The analysis method used is a combination of the Successive Corrections Method (SCM) and analysis of Cressman (1959) and the Fields by Information Blending (FIB) methodology of Holl and Mendenhall (1971), which is based on techniques using the calculus of variation suggested by Sasaki (1958, 1970).

The particular program used was developed by ANMRC for research purposes and is an extention to three dimensions of the two-dimensional objective variational analysis system used operationaly by the Australian Bureau of Meteorology, described by Seaman et al. (1977).

Two characteristics make it particularly suitable for the objective analysis of satellite temperature profiles. First, geopotential thickness is a primary analysis variable, and this makes the scheme, in the terms of Anthes and Keyser (1979), a "wind from mass" scheme. Since the satellite derived profile data are related to mass rather than wind, such an scheme is essential if these data are to be usefully assimilated into an objective analysis. Second, differing weight can be given to scalar and gradient geopotential information during the variational blending procedure which determines the geopotentials, thus allowing the geopotential gradient information inherent in the satellite temperature data sets (Schlatter and Branstator, 1979) to be utilized more effectively than would be the case in a simple SCM analysis scheme.

The wind fields are derived from the geopotential fields (in the absence of any observations of wind) by first deriving wind components using the gradient wind law (assuming that the geopotential contours have the same curvature as the trajectories), and these wind components are used as input to a variational blending procedure (see Seaman et al., 1977) to derive a stream function field at each analysis level. This stream function is used for model initiation purposes. That is, the model commences its integration from a non-divergent initial state. If observed wind data are available, the gradient wind components calculated from the geopotentials are used as first guess fields for an SCM analysis of the west-east and south-north wind components, and, in this situation, it is these analyzed wind fields which are used as input to the variational derivation of the stream function. (Principle features of the analysis system are summarized in Table 1.)

4.3 Forecast model

The forecast model is a development of the Australian Region Primitive Equations model (ARPE) which has been comprehensibly documented by McGregor et al. (1978) and extensively tested operationally with a horizontal resolution of 250 km by the Australian Bureau of Meteorology. In a research mode , the model is utilized by the ANMRC at a 125 km resolution. Performance of the model has been extensively described by Leslie et al. (1981) and it principle features are summarized in Table 1.

The current SSEC-NESDIS/DL version of the model differs in several important respects from the ANMRC version. As mentioned, the horizontal resolution has been upgraded to 67 km to make it compatible with the resolution of satellite sounding information. A finite difference scheme devised by Corby et al. (1972) to minimize truncation errors due to steep topography has been included. This was not found to be important in the relatively flat Australian region but was very important in the steep topographic regions of the continental U.S. and Canada. A Kuo-type convective parameterization (Kuo 1965, 1974) has replaced the Arakawa-Schubert scheme described in McGregor et al. (1978). Lastly, a much more comprehensive planetary boundary layer scheme has been included in the code. The scheme includes stability-dependent eddy vertical diffusion in the PBL (Blackadar 1974) for heat momentum and moisture, a similarity-theory surface layer (Businger, 1981) a description of the effects of atmosphere and clouds on the surface radiant flux (Katayama, 1972; Paltridge, 1976) and a surface energy balance equation.

5. MODEL RESULTS

5.1 Initial development of the North American region system

Three separate data sets were provided by SSEC for the ANMRC to use in the development of the North American Region analysis prognosis system. The first two cases came from the Data System Tests (DST-5) period of August 1975, and they contained data from the Nimbus-6 satellite as well as conventional radiosonde data, while the third case came from March 1979. The satellite data in this third case was obtained from the TIROS-N satellite, and these data had much higher horizontal resolution.

It is necessary to provide fields of geopotential height, temperature, and dewpoint depression at each standard pressure level, and of mean sea level pressure, at each grid point in the analysis domain for use in the generation of preliminary fields for each of the SCM analyses. Ideally, these fields come from a high quality prediction in order that the temperature and mass fields be mutually consistent. Alternatively, an analysis from a short time earlier may be used, or a climatological field could be employed. The only realistic choice, given the resources available to ANMRC at the time, was to use a climatological field. Latitudinal mean values of MSLP, geopotential height, temperature and dewpoint depression were obtained from Crutcher and Meserre (1970) and interpolated to the analysis grid.

Analyses were prepared using each of these three data sets. Each case was analyzed using all available data, and also excluding the satellite data. After some experimentation with pass radii for use in the SCM phases of the analysis, and also some changes to the weights used in the variational blending procedure (made necessary by the change in resolution of the analysis grid from that used in the Australian region versions of

the code), the analysis scheme was subjectively assessed to be producing analyses which were meteorologically consistent, and objectively assessed to be satisfactorily fitting the observations. It was observed, however, that the wind fields tended to have rather more noise than was usual in the coarser resolution analyses. During initial testing, this was allowed to remain, rather than risk unduly smoothing the fields and, thus, possibly losing the detail that the high resolution grid was intended to resolve.

All data used in the analysis of a given field were given equal weight--that is, no attempt was made to differentiate between radiosonde and satellite data in the SCM analyses of thickness, temperature or dewpoint. In addition, while all the radiosonde and upper wind data were contemporaneous, considerable aynopticity was allowed during these initial tests in the acceptance of the Nimbus-6 satellite data, with up to eight hours asynopticity being accepted between the conventional data base and the data from the final (western) orbit of the Nimbus-6 satellite over the analysis region. These two factors considerably degraded the fit of the analyses to the radiosonde data when satellite data (in particular the Nimbus-6 data) were included in the analyses.

Initial testing of the prognosis model took place on the Australian CDC CYBER-76 computer. Due to the limitations on available core on this machine, the model could only be integrated with a vertical resolution of four levels. In spite of this, 24-hour prognoses were computed from each of the three analyses in order to test the working of the North American Region version of the model.

In two of these cases the prognoses were considered successful, although with some noise close to the ground in regions of high topography, and also a significant loss of wind speed in the jet stream. Both these problems were considered to be due to the lack of vertical resolution.

Prognoses computed from the analyses of Figure 2 (a-b) are shown in Figures 3(a-b). It can be seen that the broad evolution of the synoptic patterns is consistent, with a region of high pressure developing over the central parts of the North American continent with a rather complicated series of low pressure systems near the Rocky Mountains.

The grid prognosis, based on the analysis for 12 GMT 14 March 1979 was considered to be unduly noisy and of little utility. The reasons for this were not immediately obvious, but it may either have been due to initialization, lack of vertical resolution in the forecast model, or due to inadequacies in the initial analysis.

Subsequent development of both the analysis system and the prognosis model took place at SSEC. The SSEC access to NCAR's CRAY-1 computer enabled the prognosis model to be integrated in its ten-level form. An added advantage to testing at the SSEC was the availability of analyses from the NMC in Washington for use as preliminary fields for the fine mesh analyses and for forecast verification, and also the availability of NMC's LFM prognoses for comparison with those produced by the fine mesh model. The LFM analyses and prognoses were also used to provide time-dependent lateral boundary specification.

The case of March 14, 1979, (the day for which the four-level version of the model produced a poor forecast) was rerun with the ten-level CRAY-1 version. Figures 4 (a-d) show sequentially the initial SSM field of MSLP, the SSM 12-hour forecast valid at 0000 GMT March 15, the equivalent LFM forecast and the NMC verifying analysis at 0000 GMT. The equivalent series of 500 mb heights is shown in Figures 5 (a-d).

As can be seen, the SSM ten-level version performs well in this case, with the two anticyclones over North America merging at the surface and the 500 mb trough near Hudson Bay deepening. The success of the ten-level

SSM in this case versus the four-level version suggests lack of vertical resolution as the problem in the four-level forecast.

5.2 April 10, 1979--A Pilot Experiment in Static Initialization using TIROS-N Satellite Data

After conversion to the CRAY-1 computer the case of April 10, 1979, (Red River Valley tornado episode) was a pilot experiment in updating the SSM with satellite derived temperature and moisture soundings.

For this case parts of two TIROS-N orbits at 2140 GMT and 2200 GMT were processed over the United States and southern Canada, extending for the Mississippi Valley west to the far eastern Pacific. Two-hundred eighty-three profiles were obtained from these two orbits, with the spacing ranging from 50 km between profiles in some areas to 200 km in densely clouded regions, such as Colorado and Nebraska.

4.2.1 The experiment

The running details of this experiment were, in part, dictated by the timing of the satellite orbits and the timing (approximately 0000 GMT) of the outbreak of severe weather in the Red River Valley. The experiment was performed in the following way: the National Weather Service LFM analysis at 1200 GMT April 10, 1979 was interpolated to the 71 x 101 CRAY model grid using a two-directional Bessel interpolation formula in the horizontal, and cubic splines in the vertical. This interpolated analysis was used to initialize a 12-hour forecast using the scale SSM. This forecast was designated the SSM forecast. At nine hours into the SSM forecast, that is, at 2100 GMT, these forecast fields were used as first guess for an analysis of mean sea level pressure (MSLP) and satellite (TIROS-N) temperature and moisture profiles. This new analysis was then used to initialize the forecast model for another integration, designated the SAT forecast, this

time of a six-hour duration. The convective parameterization package was not included in either forecast. Verification emphasis for the SAT forecast was in two parts. The first was comparison with the SSM and LFM forecasts at 0000 GMT, and with the LFM analysis at that time. The primary purpose of this part of the verification was to assess whether the re-initialized SAT forecast was producing synoptically reasonable and accurate fields after such a short period. The second, and more important, part of the verification process was the comparison of the evolution of the model forecast between 0000 GMT and 0300 GMT with observed conditions in the area of the severe weather outbreaks, where the network three-hourly radiosonde observations could be used. As the SAT forecast was initialized with non-divergent initial conditions, a careful assessment was made of surface pressure and vertical motion tendencies from time step to time step at individual grid points to determine if spurious external gravity waves were contaminating the results. It was found that with five-minute time steps, any surface pressure oscillations were less than 0.5 mb after 12-15 time steps, and vertical motion tendencies were also smoothly varying after a similar time.

Two variations to this experiment were also performed. In the first the convective parameterization package was included in the six-hour forecast from the 2100 GMT analysis of satellite data. A second variation was to decrease the number of satellite temperature profiles so as to increase the spacing between the observations by some 2.5 times. In this report we describe only on the main experiment, the SAT forecast, since differences between this forecast and the Kuo and reduced resolution experiment were minimal. Details of these experiments are described in Mills and Hayden (1983).

5.2.2 The SAT forecast

Figures 6 (a-f) show the MSLP fields from the LFM analysis for 1200 GMT April 10 and 0000 GMT April 11, 1979, the 12-hour LFM forecast, the SSM forecast, the 2100 GMT SAT analysis and the three-hour SAT forecast. All forecasts are valid at 0000 GMT. Much of the discussion to follow will be concerned with the Texas/Oklahoma area where the severe weather outbreak occurred, both because this is the most "interesting" (or active) area of the forecast domain, and also because it is well within the area of the chart covered by the TIROS-N data. Both the LFM (c) and the SSM (d) forecasts have similar characteristics in terms of the movement of the low pressure system but with the SSM slightly retarding the trough over Texas as compared with the LFM. This has the result that the SSM is more accurate in eastern Texas, while the LFM is more accurate in western Texas and New Mexico. In absolute magnitude, the SSM has failed to capture the deepening of the center and therefore missed the intensification of the gradient to the northeast. The SAT forecast (e), which does, of course, have the advantage of later data, is more accurate than either, with regard to both the position of the low pressure center and to the axis of the developing trough which extends from the low center through Big Bend in southern Texas. This is not purely a function of the surface data at 2100 GMT (although it undoubtedly helps) as there is a marked negative insallabaric tendency from the Texas Panhandle southwards forecast by the SAT case. The SAT forecast suffers somewhat in the east where the ridge is deflated more than was observed.

Figure 7 shows an equivalent set of 1000-500 mb thickness analyses and forecasts corresponding to Figure 8. Careful examination of these charts shows that each of the three forecasts has a major error over the Big Bend

area of Texas--that is, all three forecasts have overdeveloped the thickness trough, with the SAT forecast being the least in error in this regard. A distinctive feature in the SAT forecast, though, is that the trough is somewhat sharper then either the LFM or the SSM forecast, and much sharper than the verifying LFM analysis. This appears to be a consequence of the sharpness of the trough in the 1200 GMT SAT analysis which the forecast model has retained. The SAT forecast has a larger (and positive) thickness error over the Gulf of Mexico than either the LFM or the SSM forecasts. This error is again a feature retained from the satellite analysis which contained retrievals which were too warm.

The 250 mb isotach charts corresponding to Figures 6 and 7 are shown in Figure 10. In the figure presented, the model results have been smoothed to correspond to the LFM analyses and forecasts which are much smoother than the original model output for either the SSM forecast or the SAT analysis and forecast. The variation in scale is due, in large part, to differences in horizontal resolution of the two schemes, and to different degrees of smoothing used in preparation of the model output. Figure 8 shows that the SSM isotachs are slightly inferior to those of the LFM forecast. The largest differences appear in the southeast where the SSM forecast has extended the jet core more than the LFM (and more than was observed) and on the west side of the trough where the SSM forecast has reduced the intensity. The SAT analysis, and the SAT forecast recover the (again erroneously) greater intensity of the jet stream maxima. Some of the larger differences between the verifying analysis and the SAT forecast are over Mexico where there is little data to verify the detail of these features. A more probematical feature of both the SAT analysis and the SAT forecast is the jet maximum over Louisiana. This is a consequence of the

increased geopotential gradient produced in this area by the previously mentioned warm bias observed in these thickness fields over the Gulf of Mexico. However, despite the deficiencies of the data, it is certainly encouraging to see that the forecast has retained the fine detail of the analysis and adjusted the detail in a qualitatively reasonable fashion.

The 850 mb dewpoint fields are shown in Figures 9 (a-f) with the visible image from GOES-4 in Figure 10. For further verification, a manual analysis of surface dewpoint over Texas and Oklahoma at 0000 GMT is shown in Figure 11. The SSM forecast has produced a much more intense dewpoint gradient ("dry-line") through Texas than has the LFM forecast. In comparison to the orientation of the dry-line in Figure 11, and of the cloud-edge in Figure 10 though, the SSM forecast has the dry-line too far to the east in southern Texas, and too far west in the Texas Panhandle. The SAT forecast has captured a good position and orientation of the dry-line, and this forecast has greatly intensified the dewpoint gradient during the three-hour period of the forecast, with marked moisture advection from eastern Texas into Oklahoma, and drying over western Texas and New Mexico.

The vertical motion fields ($d\sigma/dt$) at the $\sigma = 0.5$ level for the SSM and the SAT forecasts at 0000 GMT are shown in Figures 12 and 13. The vertical motion field calculated from the SESAME RAOB network by Moore and Fuelberg (1981) (MF) is shown in Figure 14. Both the SSM and the SAT forecasts generate upward vertical motion over the general area of the Red River Valley; however, the SAT forecast corresponds much better to the independent verification of Figure 14 than does the SSM case, with the maximum upward motion being over western Oklahoma. The SAT forecast shows a second maximum in southern Texas which is not confirmed by MF. Figure 15

shows the SAT forecast vertical motion 0300 GMT 11 April (e.g., six hours into the forecast period) with the verification from MF in Figure 16. Both fields show a double maximum at this time. During the three hours from 0000 GMT, the forecast area of strongest vertical motion has moved from western Oklahoma northwards into Kansas, and it has weakened somewhat. This evolution agrees very well with the verification of Figures 14 and 16. The other area of upward vertical motion in the SAT forecast has moved into central Texas and strengthened. Although it is considerably to the south of the second maximum shown in MF, radar summaries (also in MF) show that a large thunderstorm area formed in central Texas between 0000 and 0300 field.

5.2.3 Conclusions on the April 10 experiment

It has been shown that, in this case study, high horizontal resolution satellite temperature data sets can be assimilated into a mesoscale numerical weather prediction model to produce short term forecasts with a good level of skill. It has been further demonstrated that the impact of these satellite data and, more importantly, of the high horizontal resolution of these data sets is small for both analysis and forecast of "synoptic" fields such as 1000-500 mb height, where the independent verification data is also relatively coarse. However, it has been shown that the benefits of high horizontal resolution satellite data in the initial state of a forecast are greater, in this case, for fields such as dewpoint and vertical motion, where large local gradients occur. The forecasts of the quantities, based on the analysis of the satellite data, shows a good level of accuracy as compared with high resolution rawinsonde data. Further, it is shown that the high horizontal resolution of the satellite data contributes to the accuracy of the forecast, through the

model's ability to retain details of the initialization. It must be remembered that these results apply only to one case. However, these initial results seem very encouraging, and they point to the potential of mesoscale models initialized from data gathered by either geostationary or orbiting satellites to provide useful forecasts of the evolution of severe storm environments.

6. SSM DEVELOPMENT--APRIL 10 EXPERIMENT TO PRESENT

In mid 1982 an IBM 4341 computer became operational at SSEC which for the first time provided the potential to run the SSM forecast/analysis system in-house. While it was necessary to reduce the grid size (Figure 1) to 51 x 61 because of the reduced computing power, the area coverage still includes most of the continental United States. The ten-level vertical resolution and 67 km horizontal resolution have been maintained. Conversion of the SSM package to the IBM was completed in December 1982. Since then the priorities of the program have been to:

1) Test forecast quality on the reduced grid and assure error-free functioning of the system on the IBM;
2) Test the PBL package to assess its impact on forecast quality;
3) Convert the software for producting VAS sounding data sets to the IBM-McIDAS and run an impact study (in a similar fashion to the April 10 experiment) for the case of July 20, 1981.

Tasks one and two were completed in January 1983. At that time, 12-hour control (no satellite data) forecasts were run beginning at 1200 GMT July 20, 1981, both with and without (only surface drag) the PBL package. The initial fields for these forecasts were produced by the analysis scheme using a global analysis field as a first-guess blended with

the 1200 GMT rawinsonde reports. The resulting 1200 GMT initialization fields very closely resembled the LFM analyses at 1200 GMT.

Both 12-hour forecasts show good quality compared to the verification LFM analysis at 0000 GMT July 21, 1981. Results from these two experiments for heights and temperatures vs. the LFM verification analysis are shown in Figures 17-22 (a-d). The superiority of the experiment with the PBL for heights and temperatures at 850 mb is especially evident.

At this writing the next step is to perform the satellite influenced forecast for July 20 and assess the impact of the data for this case.

7. PROGRAM DIRECTION

Beginning in May 1983, a calaborative effort between the VISSR Atmospheric Sounder (VAS) program and the National Aeronautics and Space Administration (NASA) Marshall Spaceflight Center will have the objective the assessment of the value of satellite data in numerical weather prediction. The tools to make progress in this area are well represented in the SSEC-NESDIS/DL facilities. Here facilities to produce the required satellite data sets now exist in combination with the modelling capability of the SSM and, independently of the SSM, in the expertise of Prof. David Houghton of the University of Wisconsin-Madison in incorporating satellite data in the Perky-Kreitzberg mesoscale model.

What is now needed is an assemblage of case studies and experience on which to base conclusions. The few studies which have been done hardly suffice as a data base on which to make general statements. Toward this goal, numerical simulations will be performed using both the SSM and the Perky-Kreitzberg model, focusing on the use of improved static

initializations provided by VAS temperature/moisture fields. As a subset of this experiment, the same simulations will be done except with the additional satellite wind measurements from both VAS thermal fields and cloud-drift winds. All tasks will be performed on two AVE/VAS cases (March 6 and April 24, 1982) and on April 26, 1982 when a severe weather outbreak occurred.

We expect that these case studies will expand the base of knowledge, which is now lacking for the evaluation of satellite data in numerical weather prediction.

TABLE 1

Principle Features of the Analysis Scheme and Prognosis Model

Analysis System

Combination of successive correction method and variational blending in three dimensions.

Ten pressure levels, p = 1000, 850, 700, 500, 400, 300, 250, 200, 150 and 100 mb.

Horizontal resolution: 67 km

Fields analyzed or derived at each pressure level:

- geopotential height
- temperature
- dewpoint
- wind components
- stream function

Prognosis Model

Primitive equations model in σ-coordinates.

Ten vertical levels at σ = 0.05, 0.15, 0.25, . . ., 0.95

Horizontal resolution: 67 km

Staggered horizontal grid (Arakawa "C" grid)

Semi-implicit time differencing (Δt = 10 min)

Similarily theory surface layer.

Stability dependent vertical diffusion of momentum, heat, moisture above surface layer through depth of PBL.

Surface shortwave and longwave flux modified by cloudiness.

Prognosis Model cont.

Surface energy balance equation.

Large-scale precipitation.

Kuo-type convective parameterization.

Updated boundary conditions.

CAPTIONS TO FIGURES

Figure 1: The analysis/forecast domains, CRAY-1 and IBM 4341 (smaller) versions.

Figure 2: (a) MSLP analysis valid 1200 GMT, 25 August 1975.

(b) 500 mb geopotential analysis valid 1200 GMT, 25 August 1975

Figure 3: (a) 250 mb geopotential analysis vadid 1200 GMT, 25 August 1975

(b) MSLP 24-hour prognosis, base 1200 GMT, 25 August 1975

Figure 4: (a) MSLP analysis valid 1200 GMT, 14 March 1979.

(b) MSLP analysis valid 0000 GMT, 15 March 1979 (NMC Washington).

(c) MSLP 12-hour forecast valid 0000 GMT, 15 March 1979.

(d) MSLP 12-hour forecast valid 0000 GMT, 15 March 1979, (LFM model, NMC Washington).

Figure 5: (a) 500 mb geopotential analysis valid 1200 GMT, 14 March 1979.

(b) 500 mb geopotential analysis valid 0000 GMT, 15 March 1980 (NMC, Washington.

(c) 500 mb 12-hour geopotential forecast valid 0000 GMT, 15 March 1980.

(d) 500 mb 12-hour geopotential forecast valid 0000 GMT, 15 March 1980 (LFM model, NMC Washington).

Figure 6: (a) LFM analysis of mean sea level pressure for 1200 GMT, 10 April 1979.

Figure 6: (b) LFM analysis for 0000 GMT, 11 April 1979.

(c) LFM 12-hour forecast valid 0000 GMT, 11 April 1979.

(d) SSM 12-hour forecast valid 0000 GMT, 11 April 1979.

(e) Satellite analysis valid 2100 GMT, 10 April 1979.

(f) Satellite three-hour forecast valid 0000 GMT, 11 April 1979.

Figure 7: (a-f) Analysis and forecast 1000-500 mb thickness in same format as in Figure 6.

Figure 8: (a-f) Analysis and forecast 250 mb isotachs in same format as in Figure 6.

Figure 9: Analysis and forecast 850 mb dewpoint in same format as in Figure 6.

Figure 10: SMS-1 and GOES-3 visible images for 2030 and 2315 GMT, 10 April 1979.

Figure 11: Surface dewpoint analysis for 0000 GMT, 11 April 1979.

Figure 12: Vertical motion (σ) at the $\sigma = 0.5$ level for the 12-hour SSM forecast valid 0000 GMT, 11 April 1979.

Figure 13: Vertical motion at the $\sigma = 0.5$ level for the three-hour SAT forecast valid 0000 GMT, 11 April 1979.

Figure 14: Vertical motion (mb sec^{-1}) at 500 mb from SESAME data at 0000 GMT, 11 April 1979 (Moore and Fuelberg, 1981).

Figure 15: Vertical motion at the $\sigma = 0.5$ level for the six-hour SAT forecast valid 0300 GMT, 11 April 1979.

Figure 16: Vertical motion (mb sec^{-1}) at 500 mb from SESAME data at 0300 GMT, 11 April 1979 (Moore and Fuelberg, 1981).

Figure 17: (a) SSM 850 mb geopotential analysis valid 1200 GMT, 20 July 1981.

(b) No PBL SSM 850 mb geopotential forecast valid 0000 GMT, 21 July 1981.

(c) PBL SSM 850 mb geopotential forecast valid 0000 GMT, 21 July 1981.

(d) LFM analysis of 850 mb geopotential valid 0000 GMT, 21 July 1981.

Figure 18: (a-d) Analyses and forecasts of 700 mb geopotential in same format as in Figure 17.

Figure 19: (a-d) Analyses and forecast of 500 mb geopotential in same format as in Figure 17.

Figure 20: (a-d) Analyses and forecasts of 850 mb temperatures in same format as in Figure 17.

Figure 21: (a-d) Analyses and forecasts of 700 mb temperatures in same format as in Figure 17.

Figure 22: (a-d) Analyses and forecasts of 500 mb temperatures in same format as in Figure 17.

REFERENCES

Anthes, R. A. and T. T. Warner, 1978: Development of hydrodynamic models suitable for air-pollution and other mesometeorological studies. Mon. Wea. Rev., 106, 1045-1078.

Anthes, R. A., and D. Keyser, 1979: Tests of a fine mesh model over Europe and the United States. Mon. Wea. Rev., 107, 963-984.

Blackadar, A. K., 1974: Experiments with simplified second-moment approximations for use in regional scale models. Select Research Group in Air Pollution Meteorology, Second Annual Progress Report, EPA-650/4-74-045, 676 pp.

Bleck, R., 1977: Numerical simulation of lee cyclogenesis in the Gulf of Genoa. Mon. Wea. Rev., 105, 428-445.

Businger, J. A., J. C. Wyngaard, Y. Izumi and E. F. Bradley, 1971: Flux profile relationships in the atmospheric surface layer. J. Atmos. Sci., 28, 181-189.

Corby, G. A., A. Gilchrist, and R. L. Newson, 1972: A general circulation model of the atmosphere suitable for long period integrations. Quart. J. Roy. Meteor. Soc., 98, 809-832.

Cressman, G., 1959: An operational objective analysis system. Mon. Wea. Rev., 87, 367-374.

Crutcher, H. L. and J. M. Meserre, 1970: Selected level heights, temperatures and dewpoints for the northern hemisphere NAVAIR 50-1C-52. U. S. Naval Weather Service Command.

Gauntlett, D. J., L. M. Leslie, J. L. McGregor, and D. R. Hincksman, 1978: A limited area nested numerical weather prediction model: formulation and preliminary results. Quart. J. Roy. Meteor. Soc., 104, 103-117.

Halem, M., E. Kalnay, W. Baker, and R. Atlas, 1982: Determination of moisture from NOAA Polar orbiting satellite sounding radiances. Bull. Amer. Meteor. Soc., 63, 407-426.

Holl, M. M. and B. R. Mendenhall, 1971: Fields by information blending, sea level pressure version. Project Rep. M167. Meteorology International, Monterey, California.

Katayama, A., 1972: A Simplified Scheme for Computing Radiative Transfer in the Troposphere, University of California at Los Angeles Technical Report No. 6, 77 pp.

Kelly, G. A. M., G. A. Mills, and W. L. Smith, 1978: Impact of Nimbus-6 temperature soundings on Australian region forecasts. Bull. Amer. Meteor. Soc., 59, 393-405.

Kuo, H. L., 1974: Further studies of the parameterization of the influence of cumulus convection on large scale flow. J. Atmos. Sci., 31, 1232-1240.

Kuo, H. L., 1965: On formation and intensification of tropical cyclones through latent heat release by cumulus convection. J. Atmos. Sci., 22, 40-63.

Lee, D. K., and D. D. Houghton, 1981: Impact of mesoscale satellite wind data on numerical model simulations. Preprints, Fifth Conference on Numerical Weather Prediction, Monterey, November, 1981. American Meteorological Society, Boston, 171-178.

Leslie, L. M., G. A. Mills, and D. J. Gauntlett, 1981: The impact of FGGE data coverage and improved numerical techniques in numerical weather prediction in the Australian region. Quart. J., Roy. Meteor. Soc., 107, 629-642.

McGregor, J. L., L. M. Leslie, and D. J. Gauntlett, 1978: The ANMRC limited area model: Consolidated formulation and operational results. Mon. Wea. Rev., 106, 427-438.

Mills, G. A., and C. M. Hayden, 1983: The use of high horizontal resolution satellite temperature and moisture profiles to initialize a mesoscale numerical weather prediction model--a severe weather event case study. To be pubished in Mon. Wea. Rev.

Mills, G. A., L. M. Leslie, and G. A. M. Kelly, 1980: A high resolution numerical analysis/forecast system for short term prediction over the North American region. ANMRC report to NOAA/NESS Development Laboratory, University of Wisconsin-Madison, Madison, Wisconsin, 53706, 73 pp.

Miyakoda, K., and A. Rosati, 1977: One-way nested grid models: The interface conditions and the numerical accuracy. Mon. Wea. Rev., 105, 1092-1107.

Moore, J. T., and H. E. Fuelberg, 1981: A synoptic analysis of the first AVE-SESAME '79 period. Bull. Amer. Meteor. Soc., 62, 1577-1590.

Paltridge, G. W., and C. M. R. Platt, 1976: Radiative Processes in Meteorology and Climatology. New York, Elsevier Scientific Publishing Company, 318 pp.

Saski, Y., 1970: Some basic formalisms in numerical variational analysis. Mon. Wea. Rev., 98, 875-910.

Saski, Y., 1958: An objective analysis based on the variational method. J. Meteor. Soc. Japan, 36, 77-88.

Schalatter, T. W., and G. W. Branstator, 1979: Estimation of errors in Nimbus-6 temperature profiles and their spatial correlation. Mon. Wea. Rev., 107, 1402-1413.

Seaman, R. S., R. L. Falconer, and J. Brown, 1977: Application of a variational blending technique to numerical analysis in the Australian Region. Aust., Meteor. Mag., 25, 2-23.

Shuman, F. G., 1978: Numerical weather prediction. Bull. Amer. Meteor. Soc., 59, 5-17.

Tarbell, T. C., T. T. Warner, and S. W. Wolcott, 1981: The initialization of a mesoscale weather prediction model using satellite and precipitation data. Proceedings, IAMAP Symposium on Nowcasting: Mesoscale observations and short term prediction, 25-28 August 1981. ESA SP-265, 259-264, Agence Spatiale Europeenne, 8-10 ru Mario-Nikis, 75738, Paris 15, France.

Wilson, T. A., and D. D. Houghton, 1979: Mesoscale wind fields for a severe storm situation determined from SMS cloud observations. Mon. Wea. Rev., 107, 1198-1209.

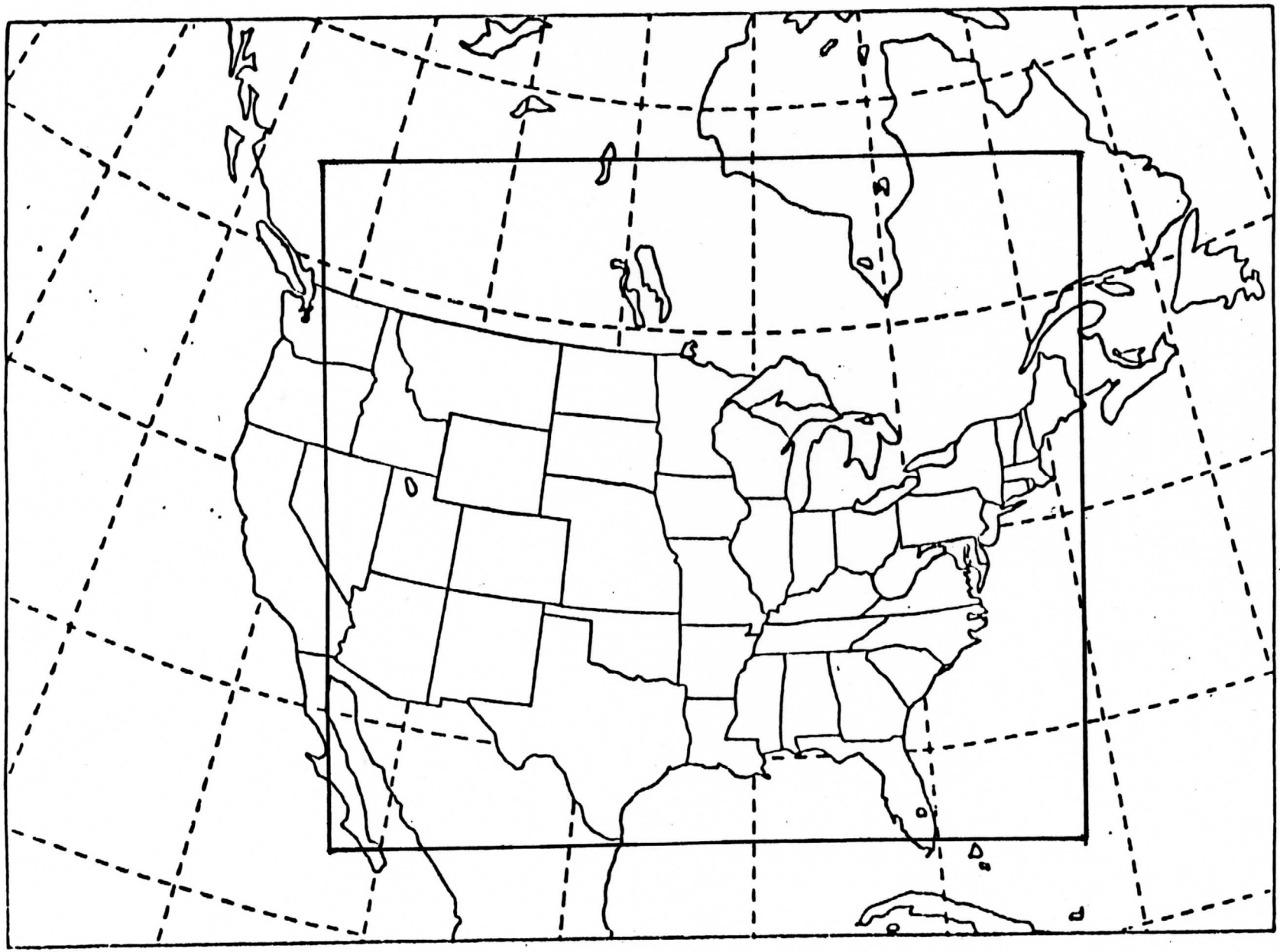

Figure 1

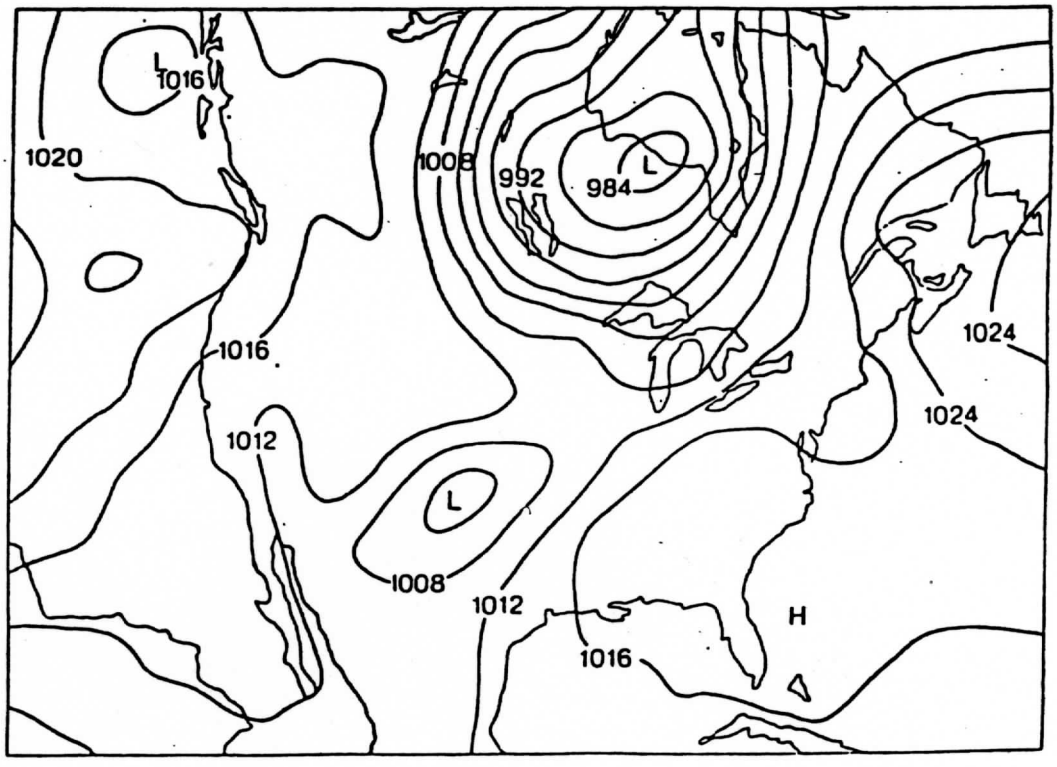

Figure 2a

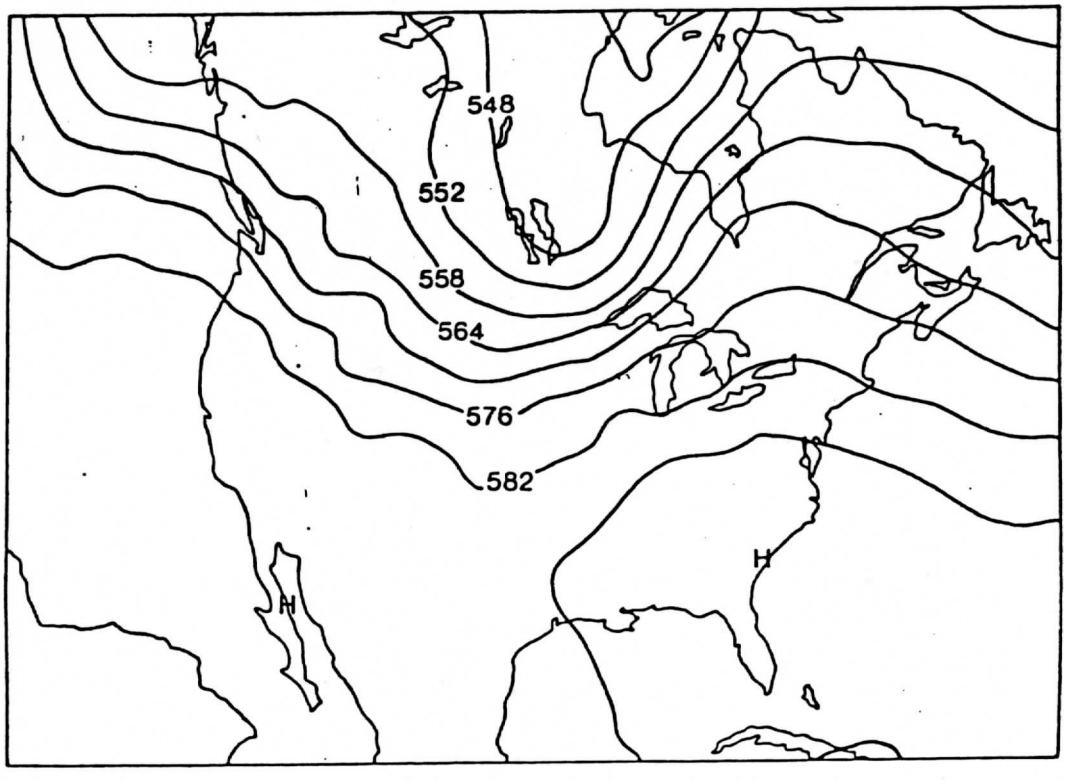

Figure 2b

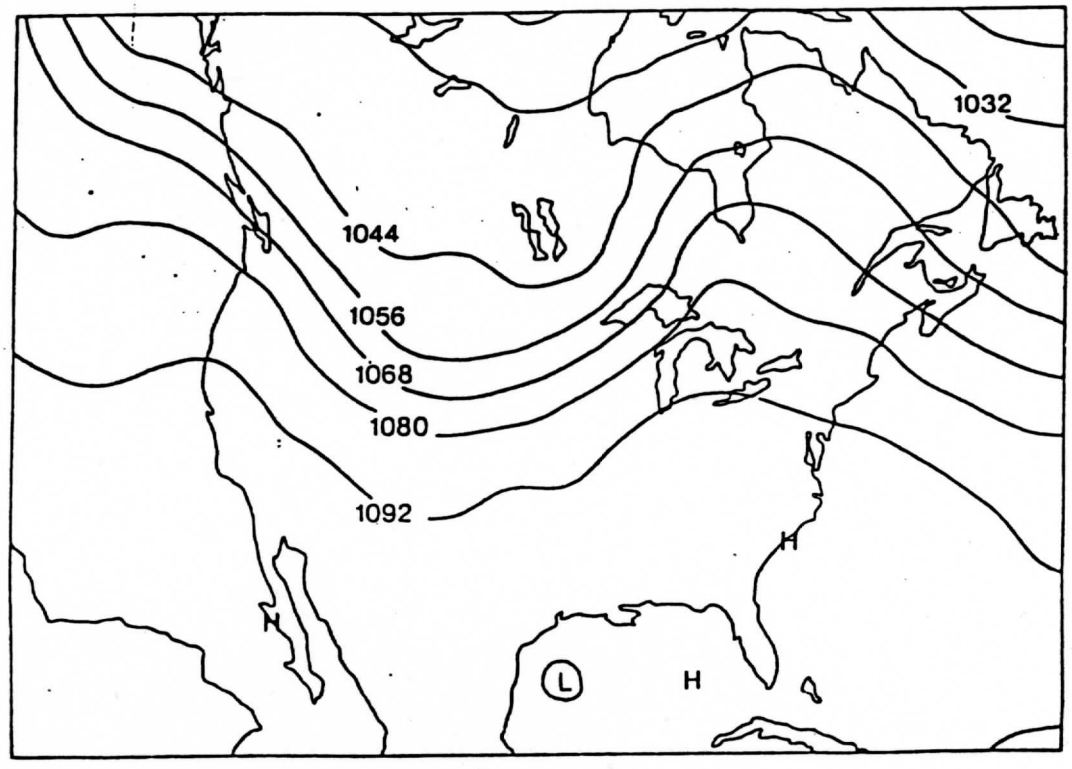

Figure 3a

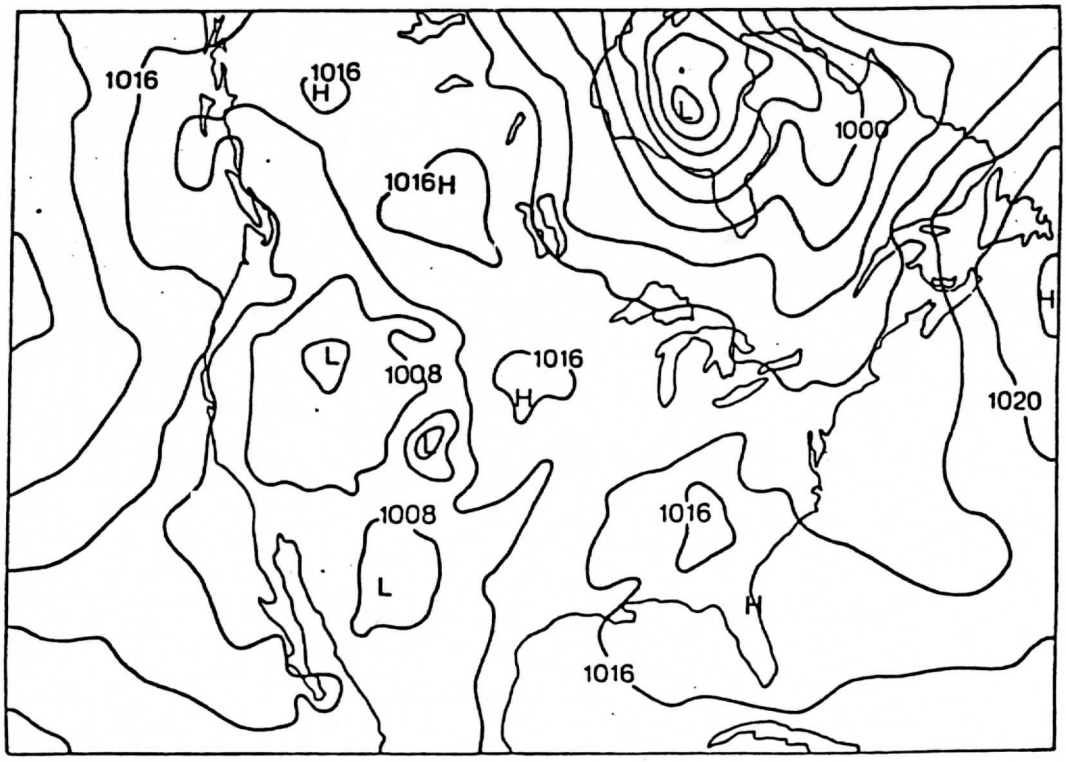

Figure 3b

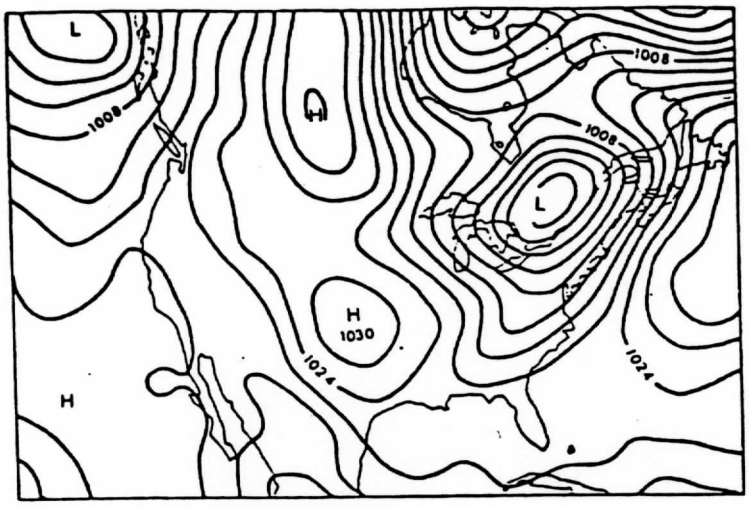

Figure 4a

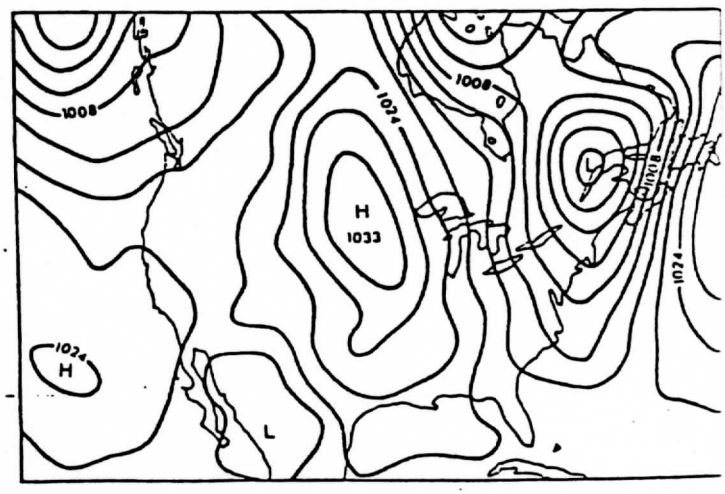

Figure 4b

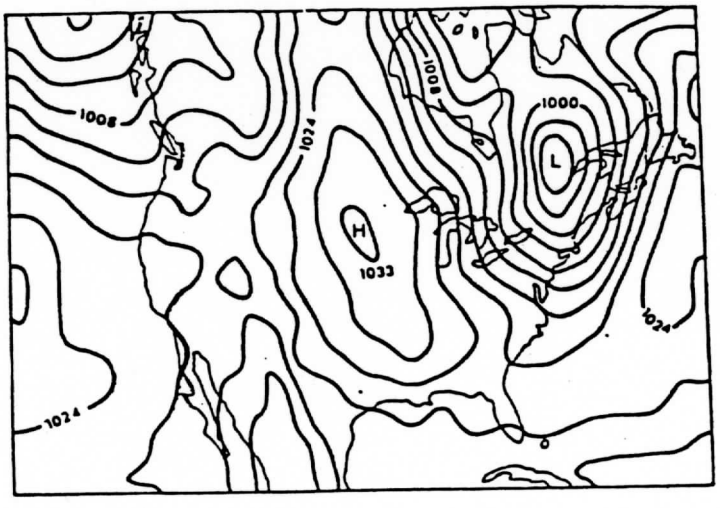

Figure 4c

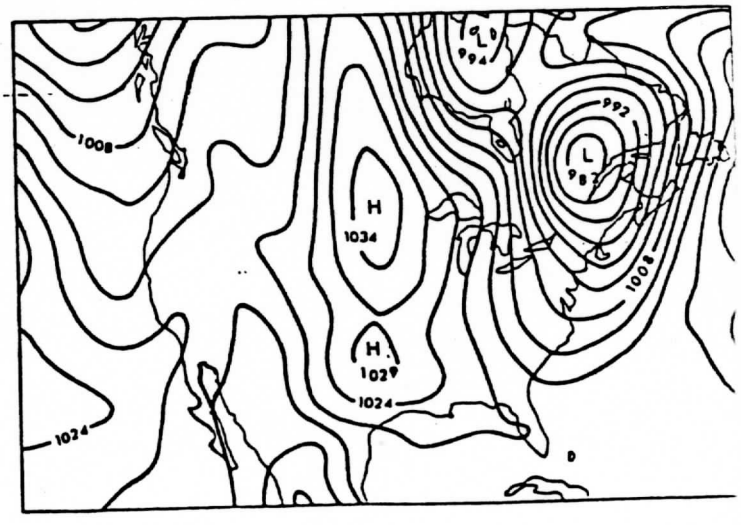

Figure 4d

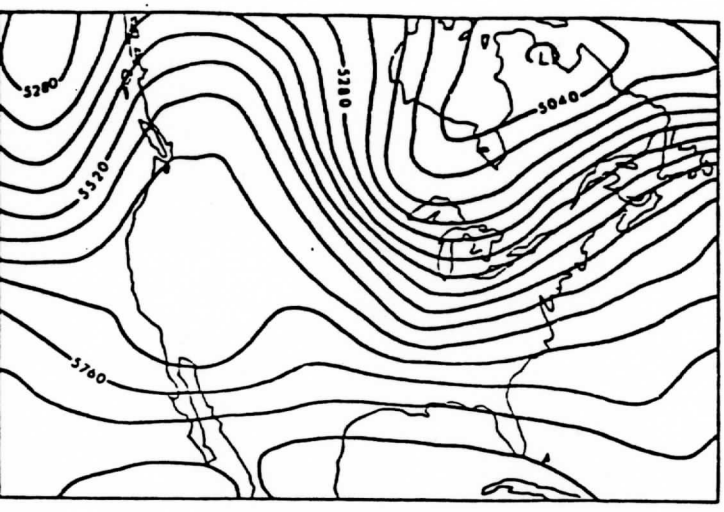

Figure 5a

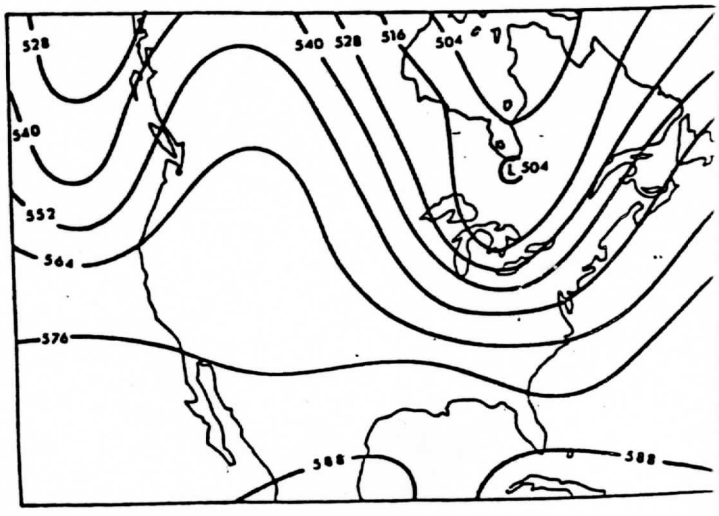

Figure 5b

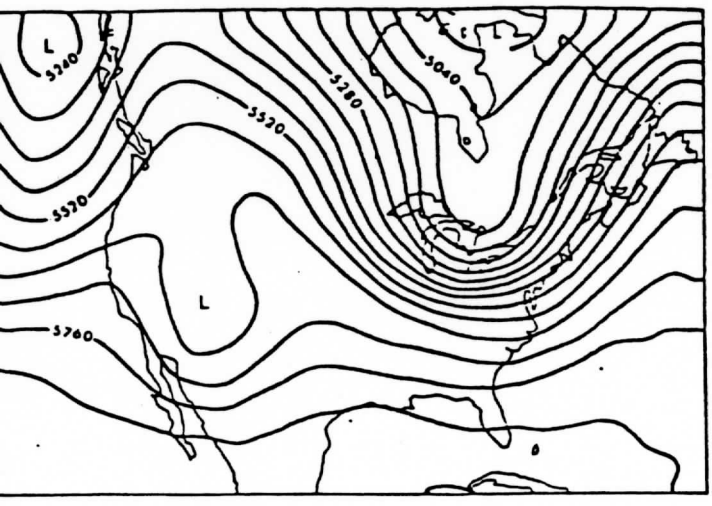

Figure 5c

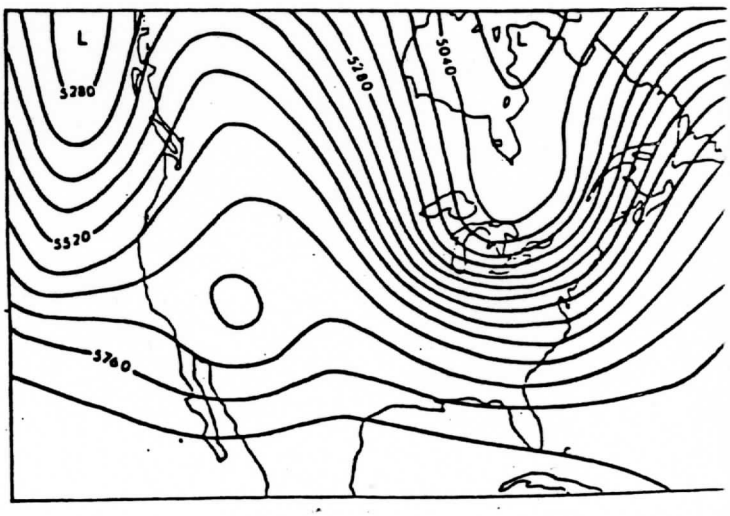

Figure 5d

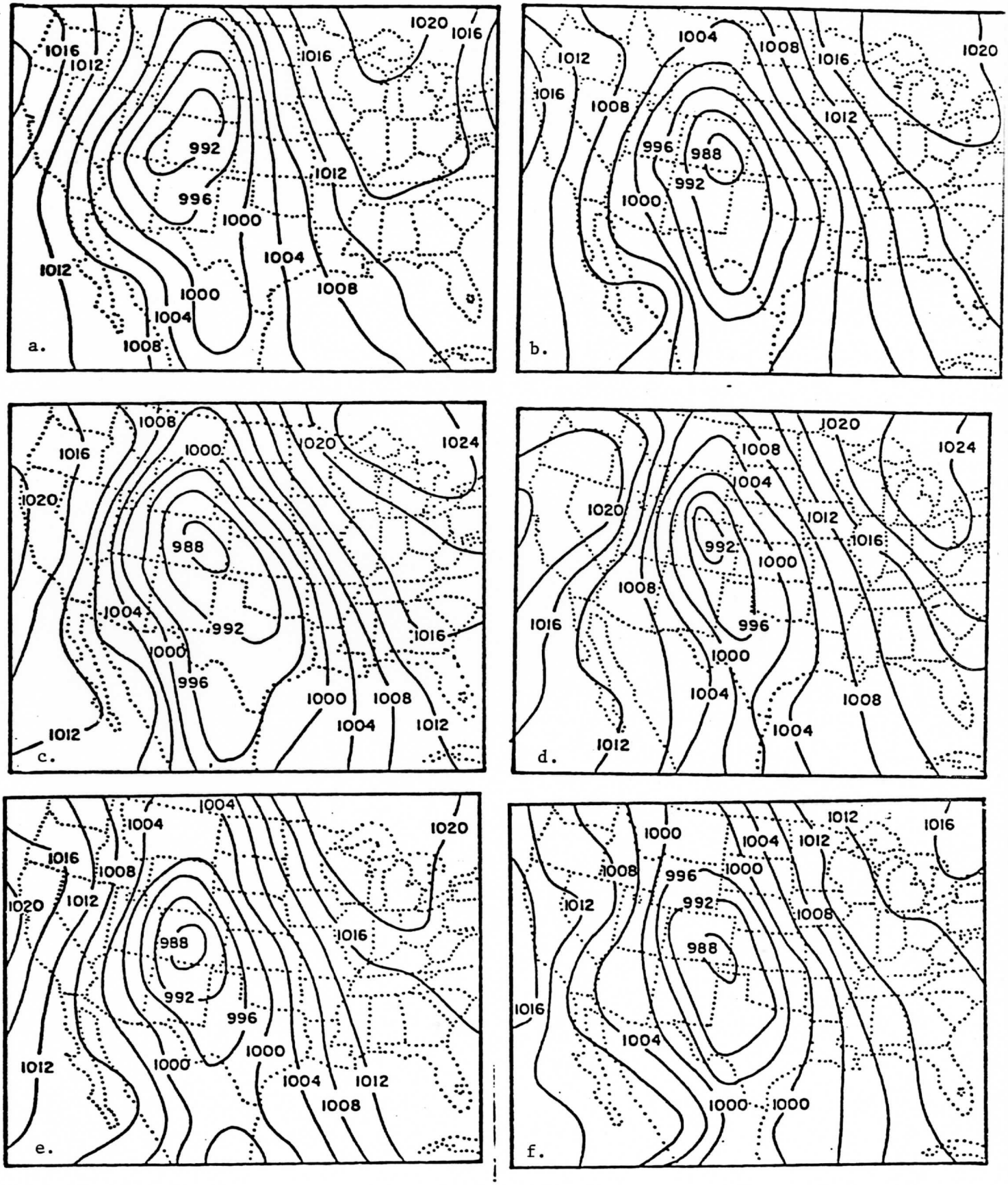
a.
1020
1016
1012
1016
992
1012
996
1000
1004
1012
1000
1004
1008
1008
b.
1004
1008
1016
1020
1012
1016
1008
1012
996
988
992
1000
c.
1008
1016
1000
1020
1024
1020
988
1004
992
1016
1000
996
1000
1008
1004
1012
1012
d.
1020
1008
1024
1004
1020
1012
1016
992
1000
1008
1016
996
1000
1004
1008
1004
1012
e.
1004
1004
1020
1016
1008
1020
1012
1016
988
992
996
1000
1012
1000
1004
1012
1008
f.
1000
1012
1016
1004
1012
1008
996
1000
1012
992
1008
988
1016
1004
1000
1000

Figure 6

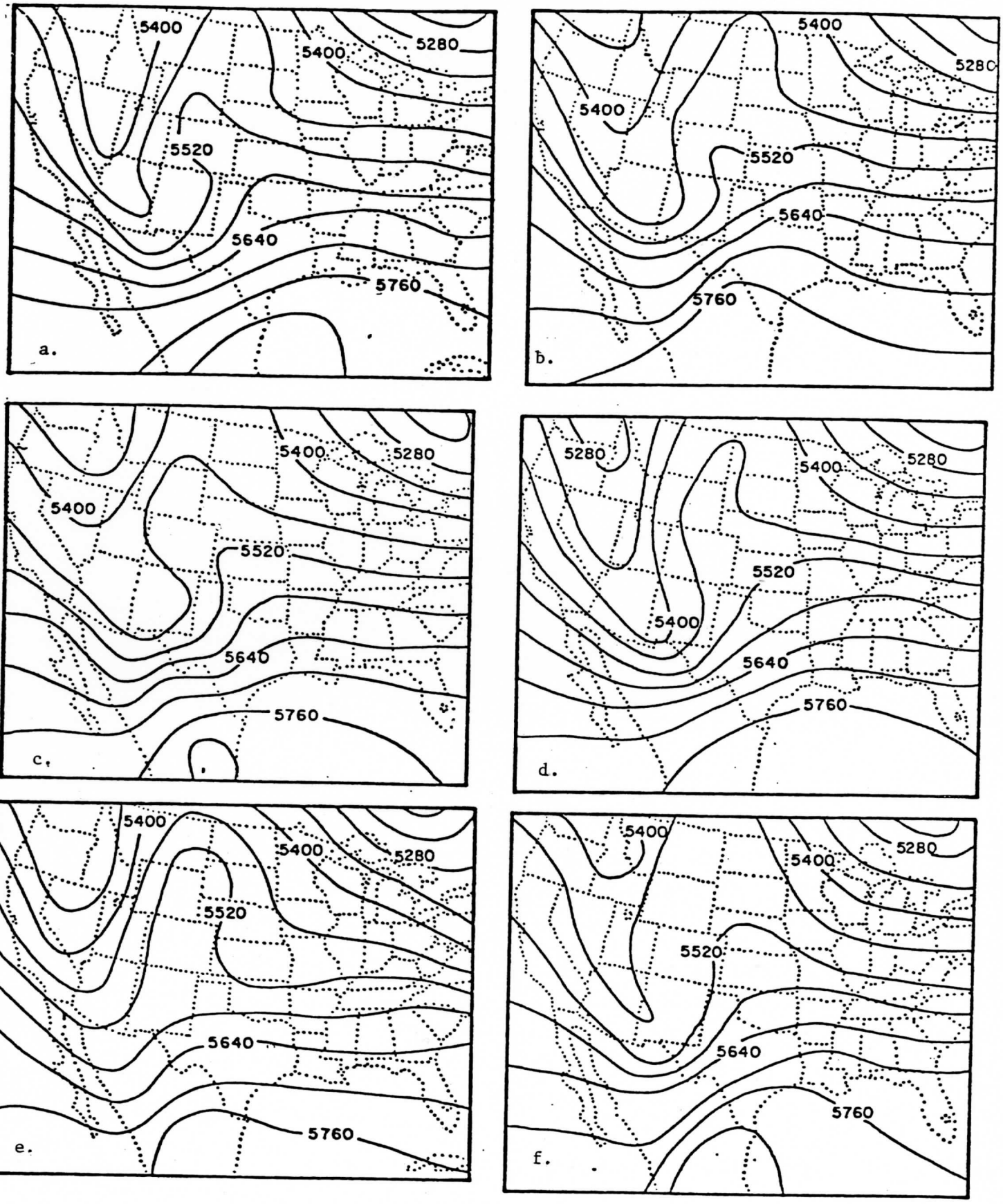
5400
5400
5280
5520
5640
5760
a.
5400
5400
5280
5520
5640
5760
b.
5400
5400
5280
5520
5640
5760
c.
5280
5400
5280
5520
5400
5640
5760
d.
5400
5400
5280
5520
5640
5760
e.
5400
5400
5280
5520
5640
5760
f.

Figure 7

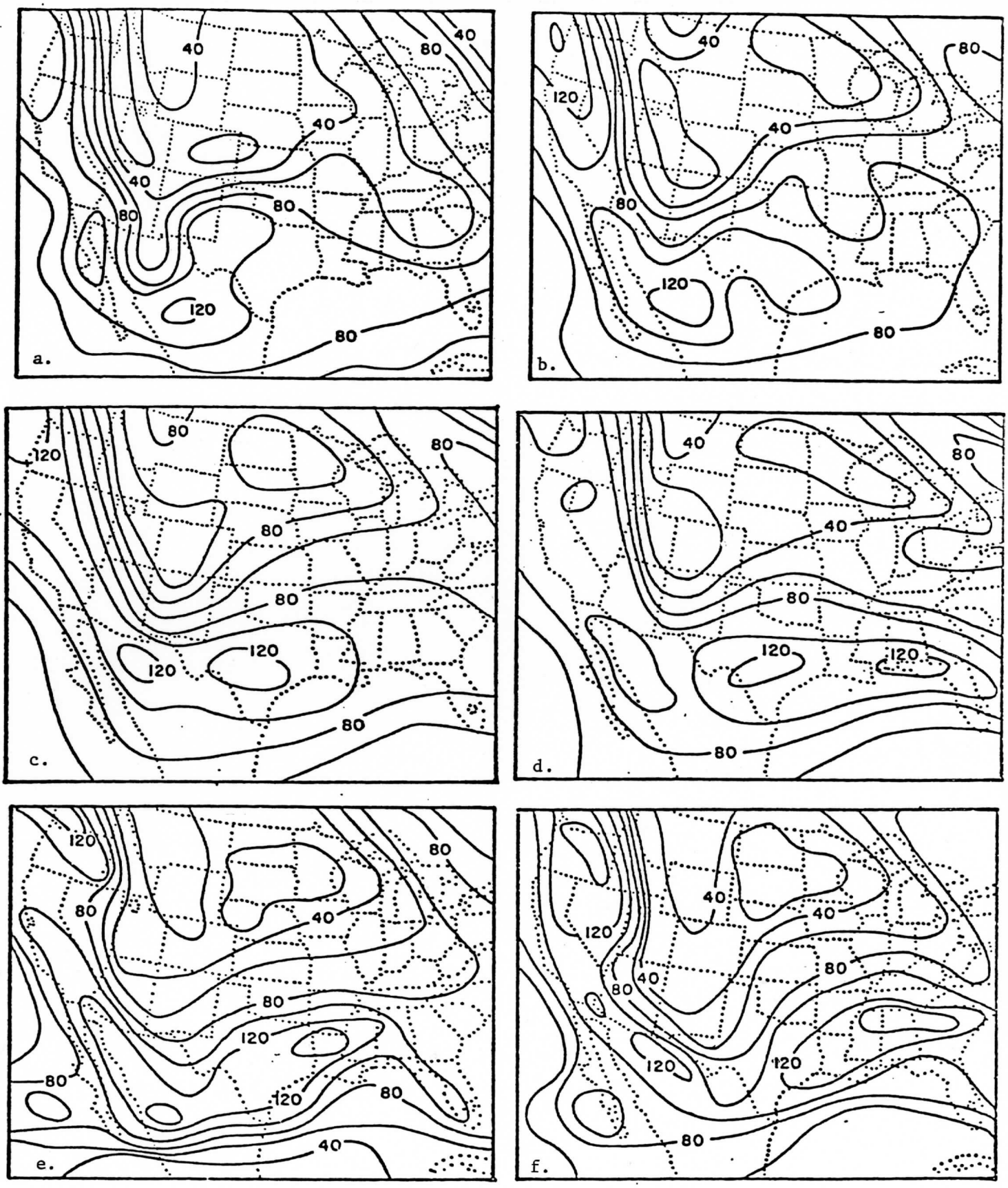
a.
40
80
40
40
40
80
80
120
80
b.
40
80
120
40
80
120
80
c.
80
120
80
80
80
120
120
80
d.
40
80
40
80
120
120
80
e.
120
80
80
40
80
120
80
120
80
40
f.
40
40
120
80
40
80
120
120
80

Figure 8

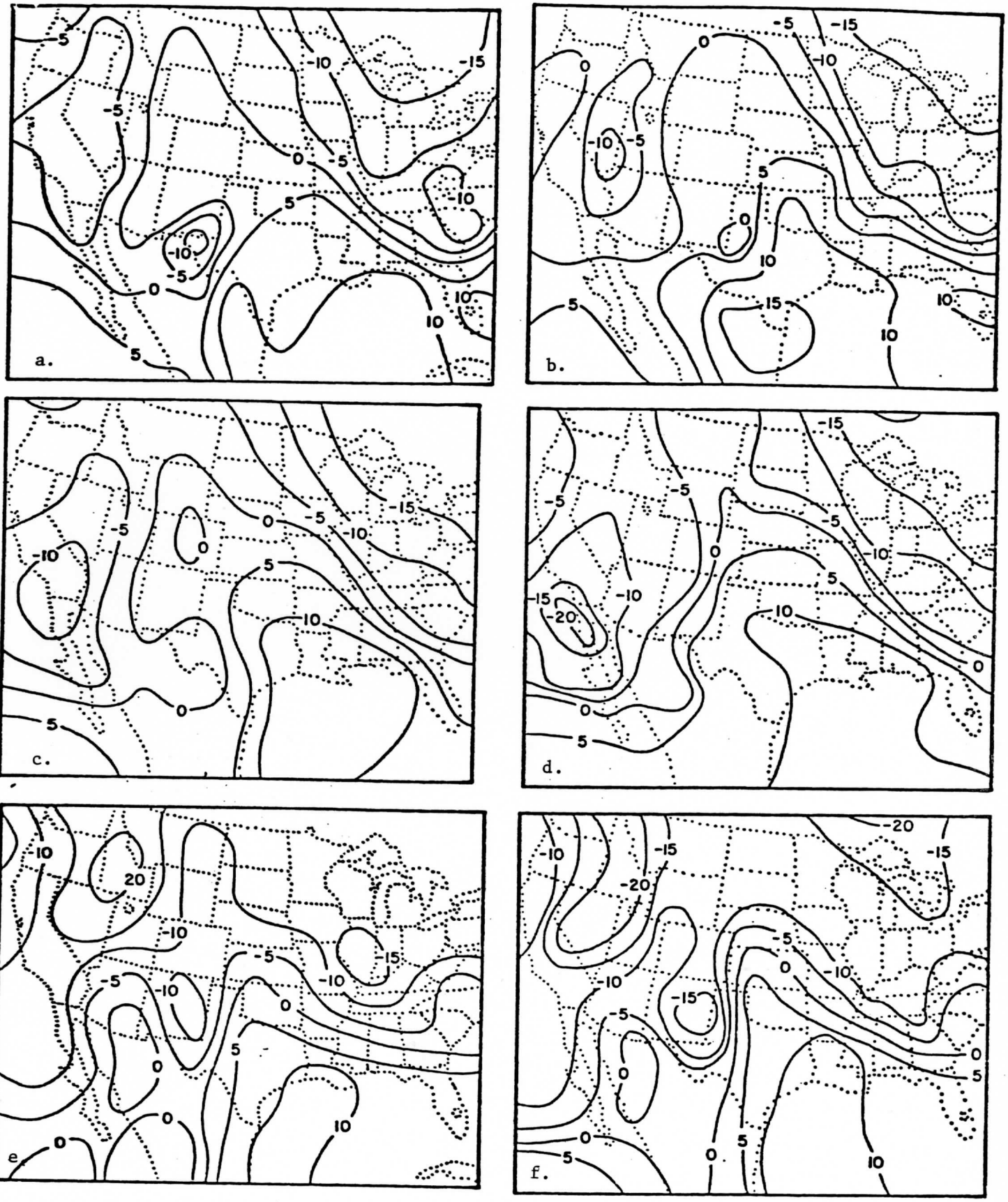

Figure 9

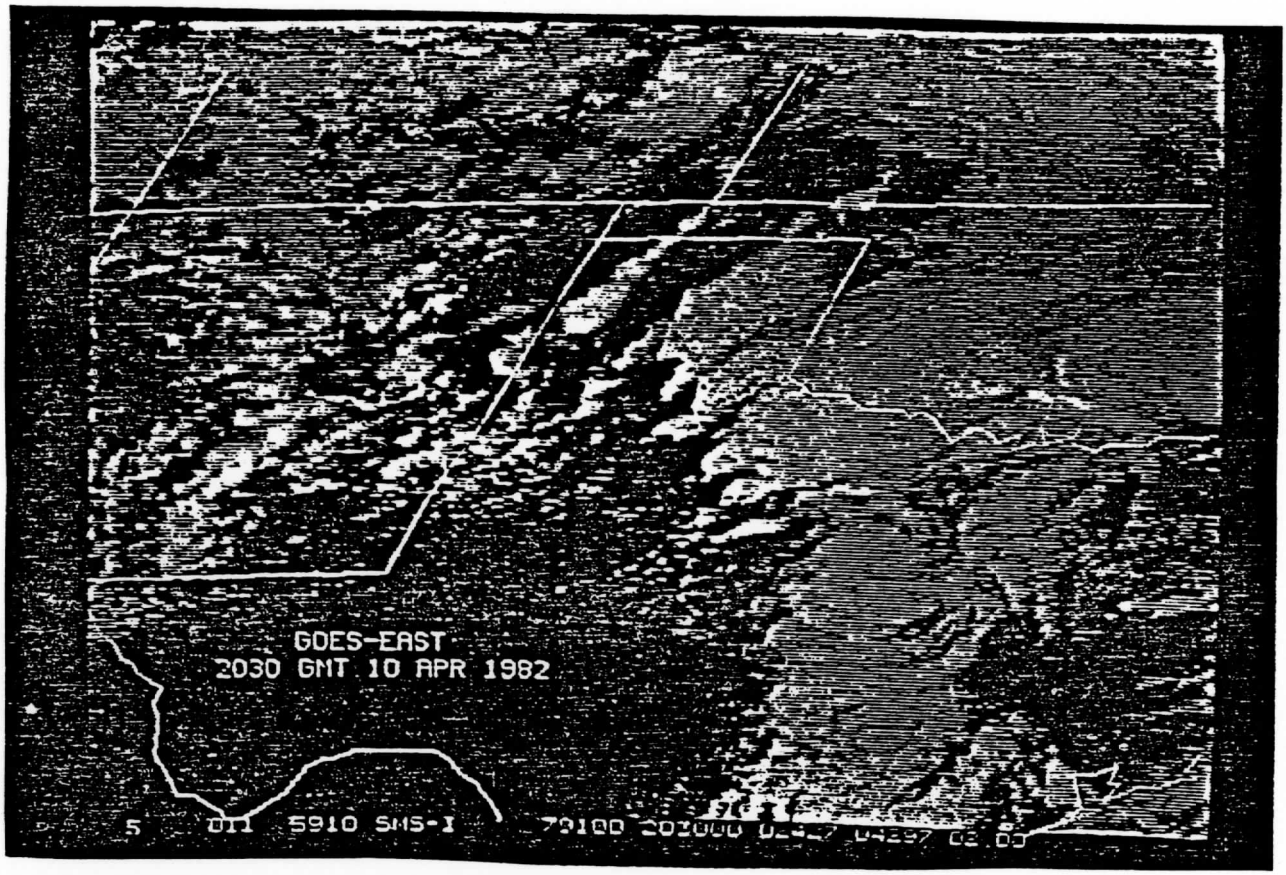
GOES-EAST
2030 GMT 10 APR 1982
5 011 5910 SMS-I 79100 202000

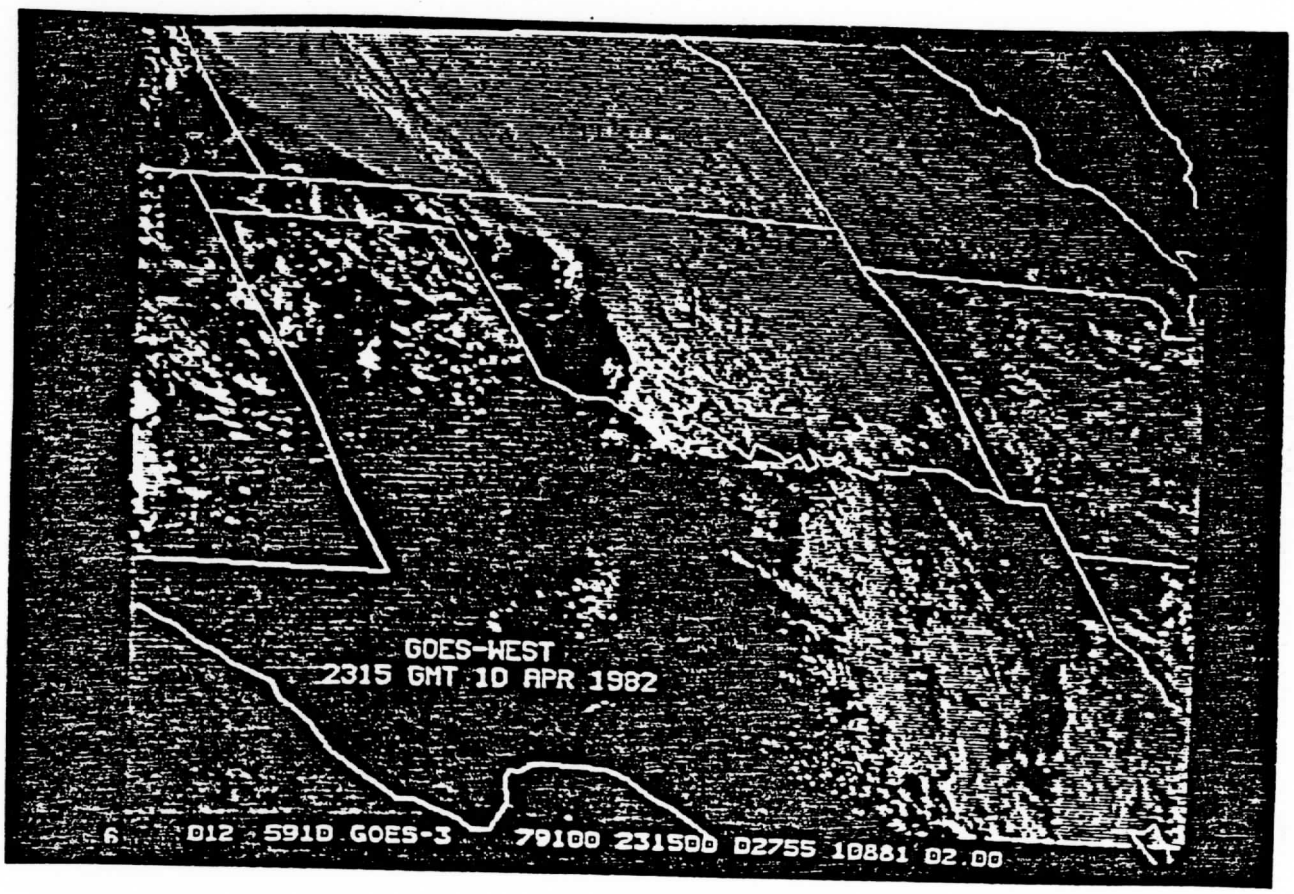
GOES-WEST
2315 GMT 10 APR 1982
6 012 5910 GOES-3 79100 231500 02755 10881 02.00

Figure 10

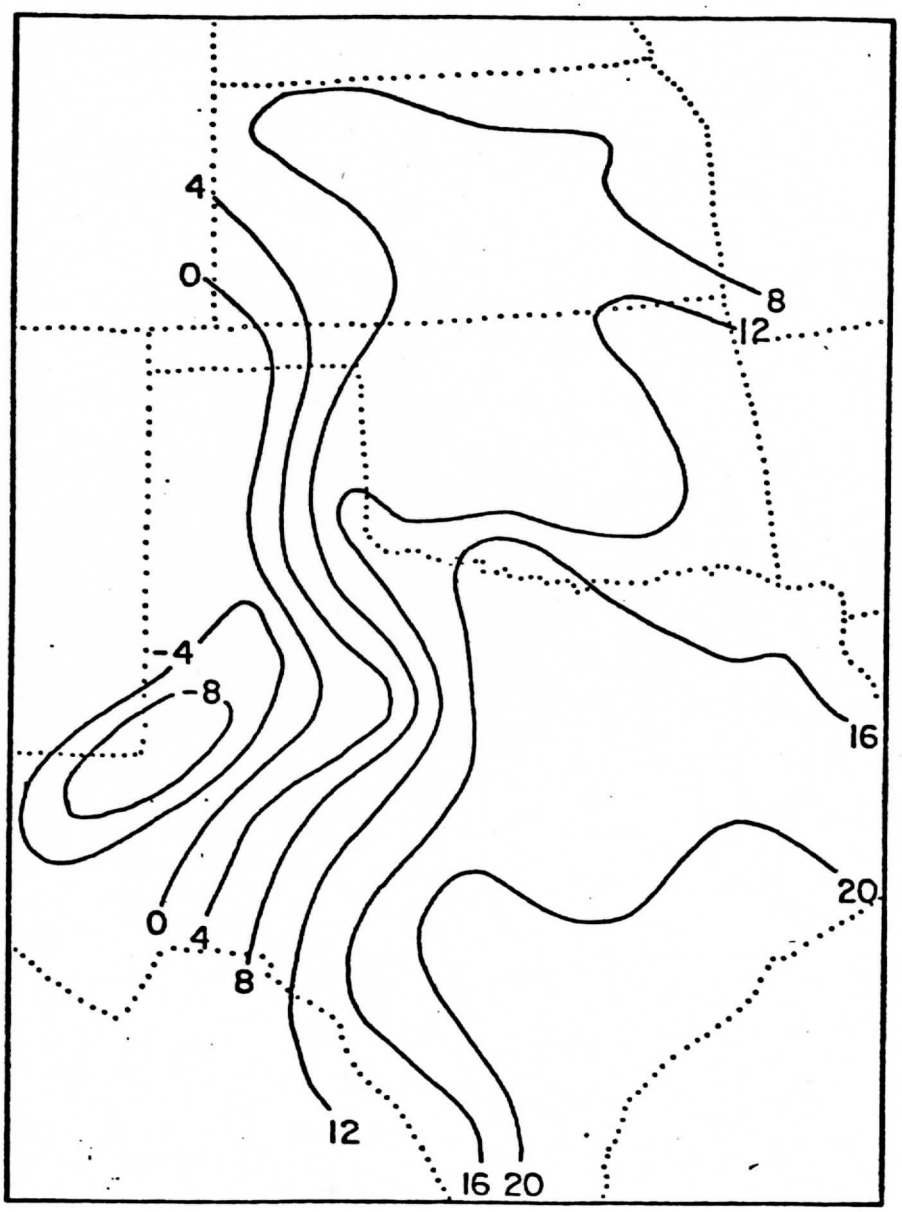

Figure 11

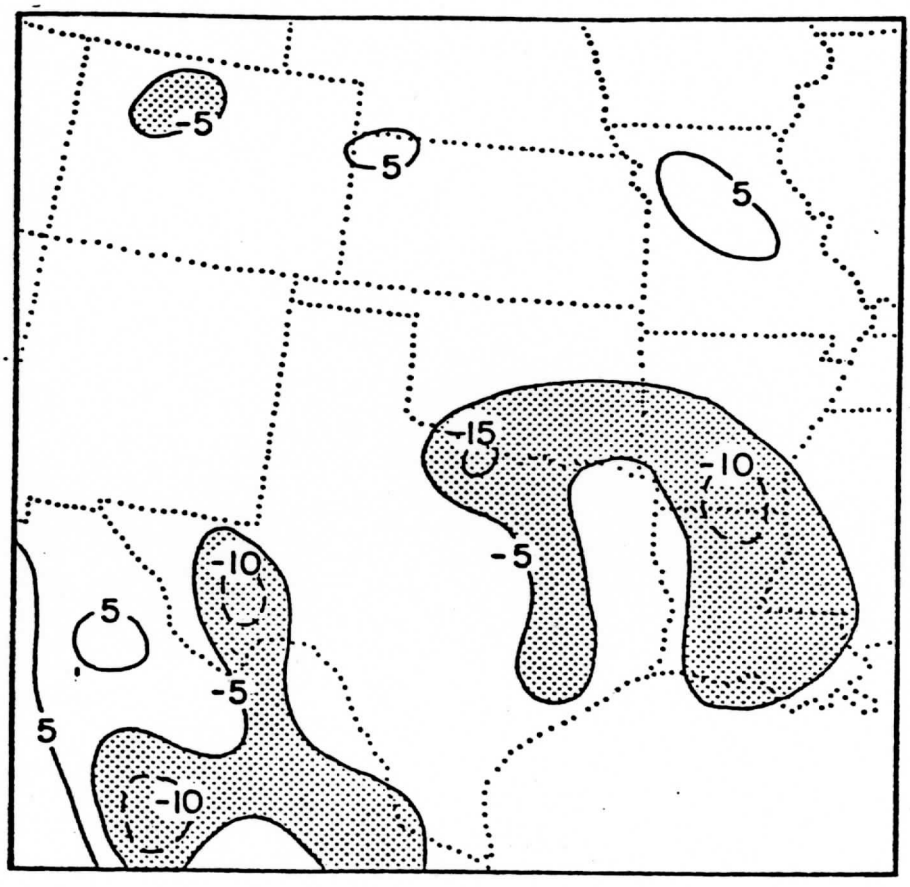

Figure 12

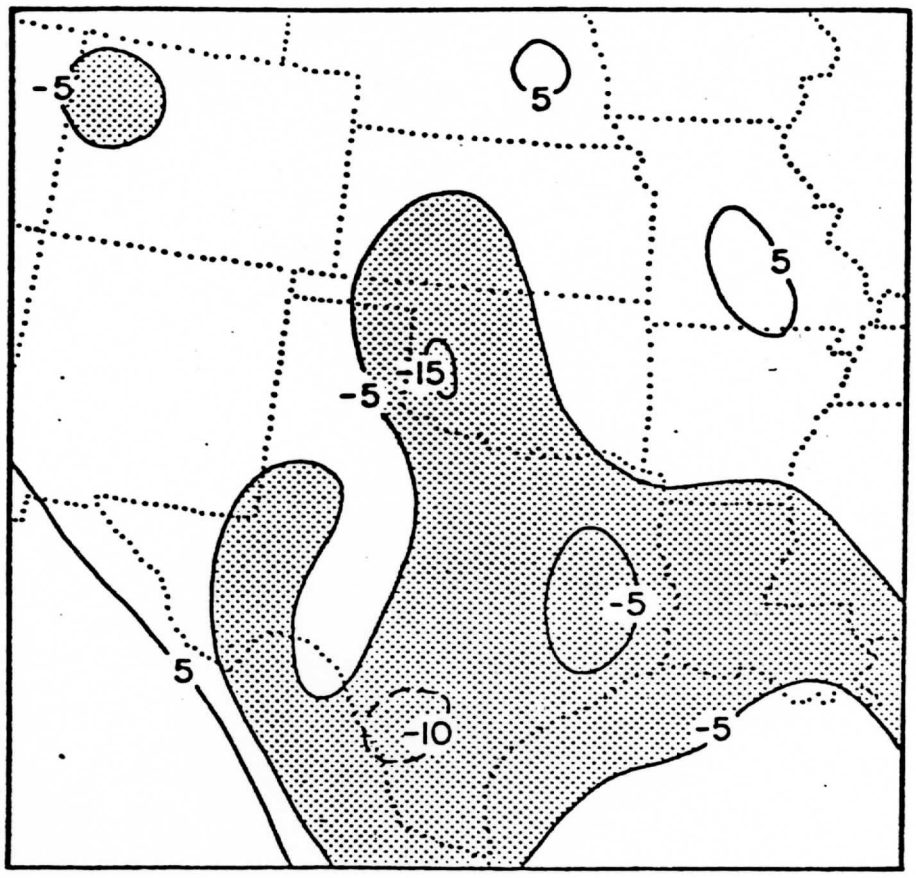

Figure 13

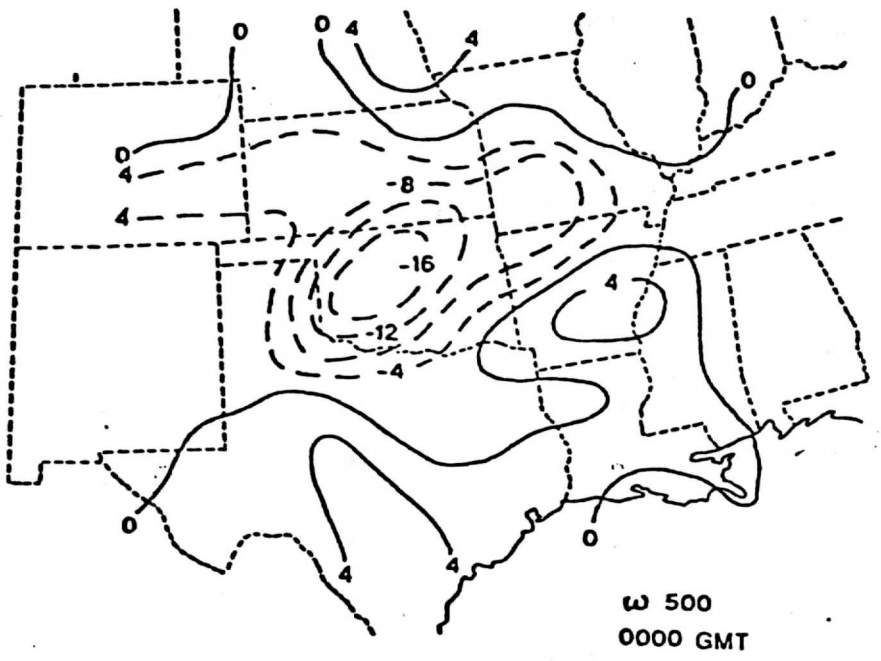

Figure 14

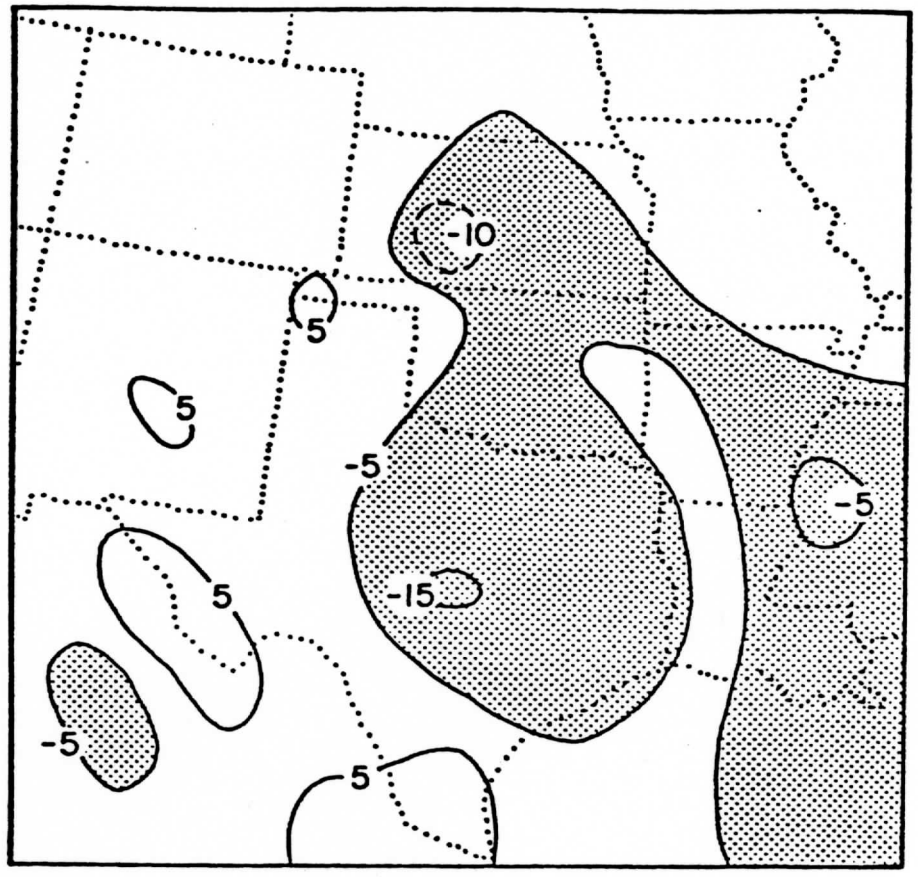

Figure 15

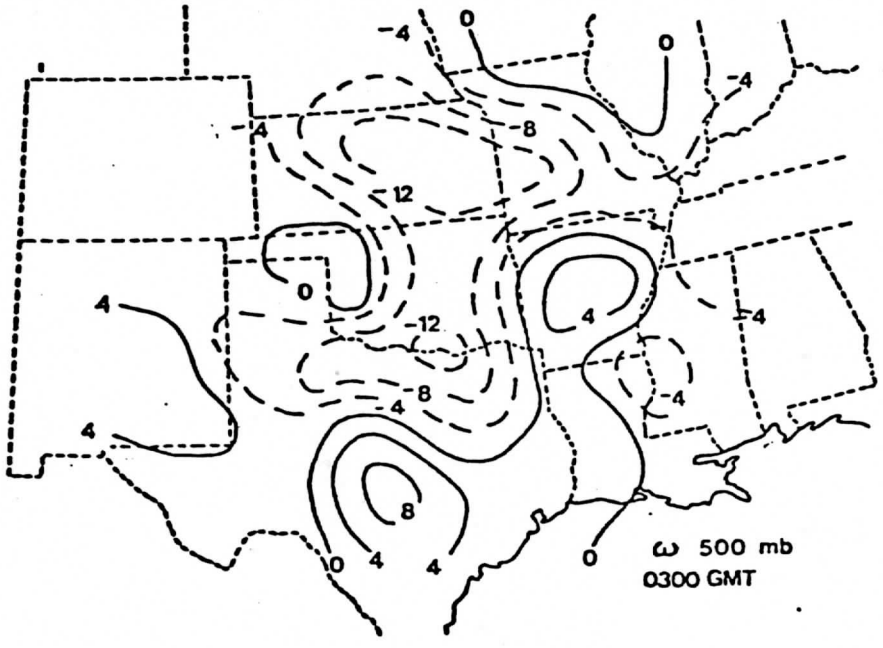

Figure 16

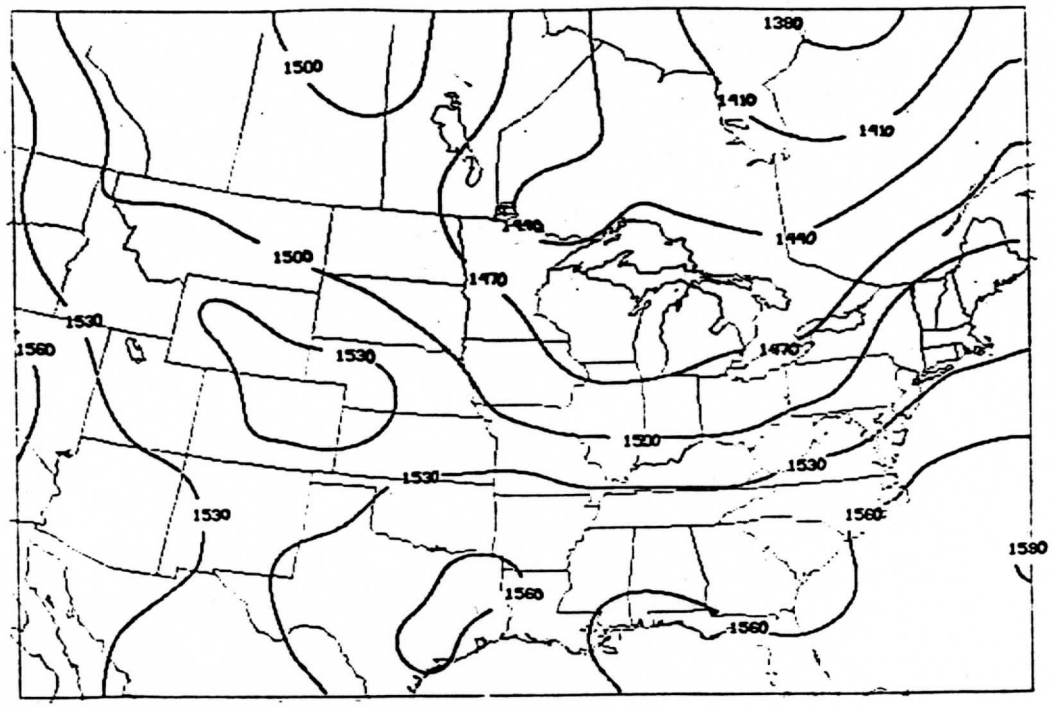

Figure 17a

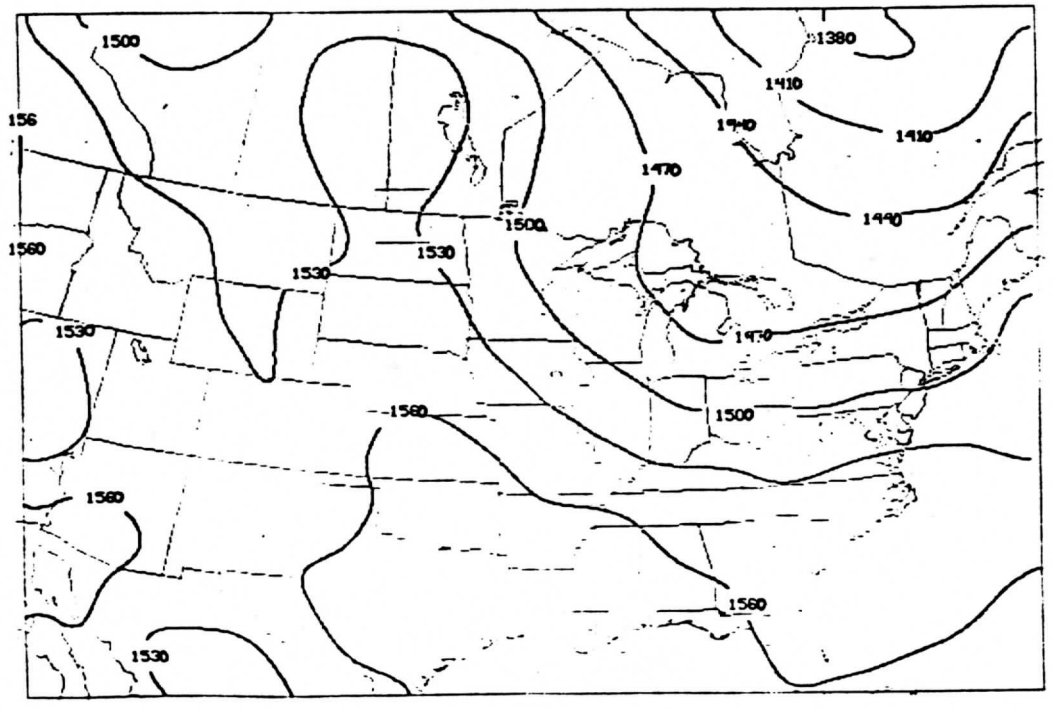

Figure 17b

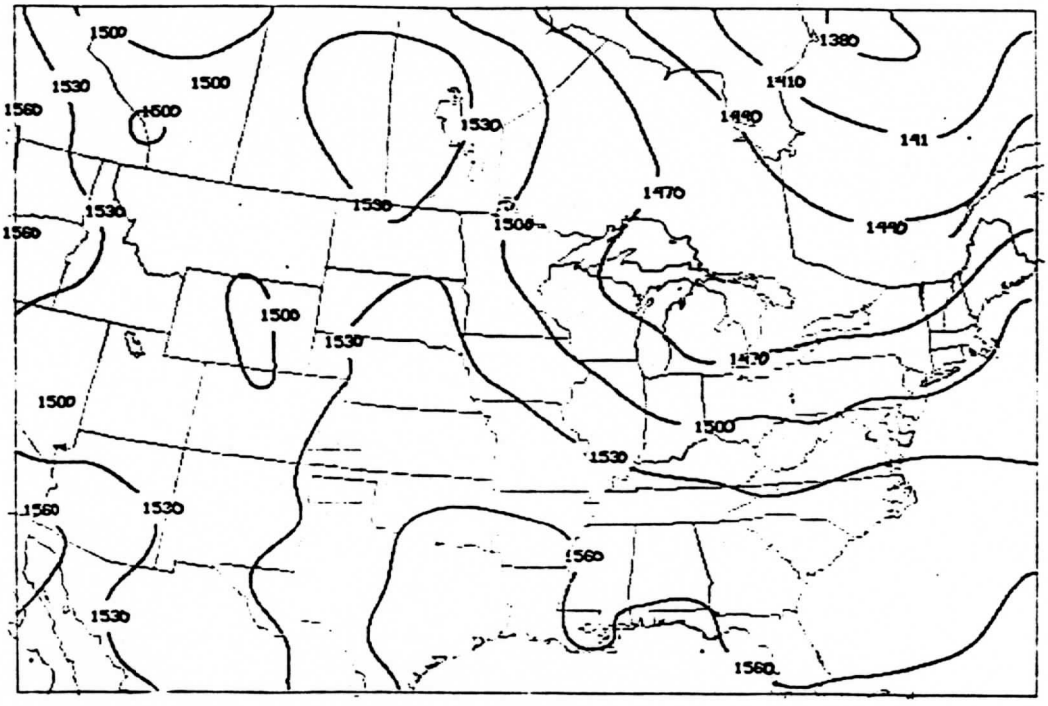

Figure 17c

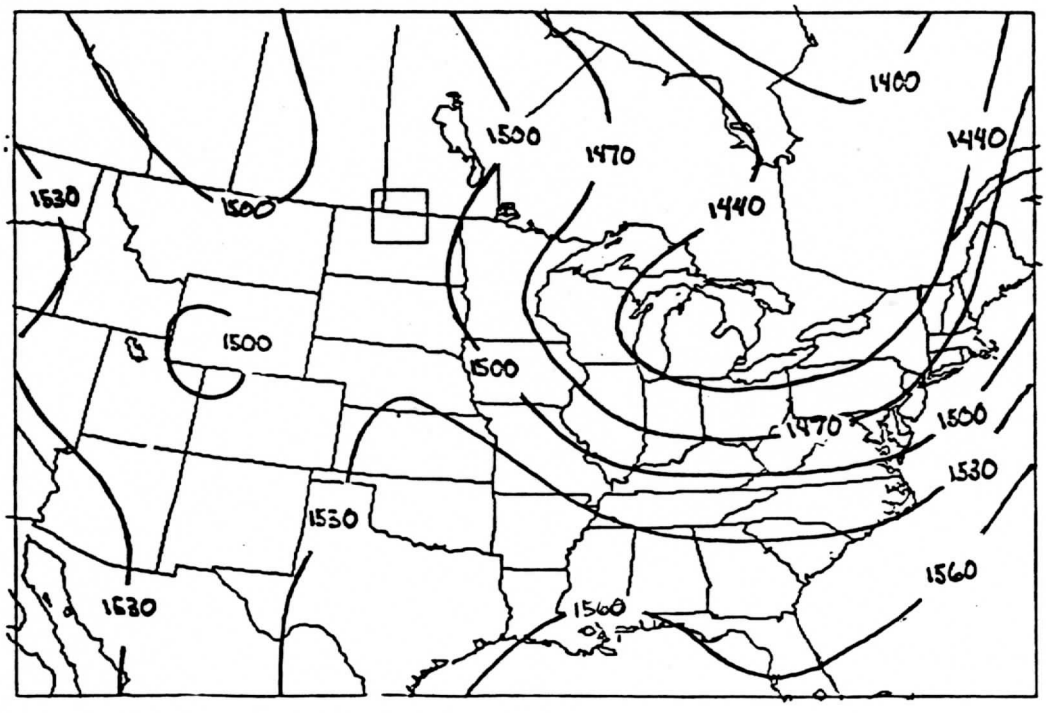

Figure 17d

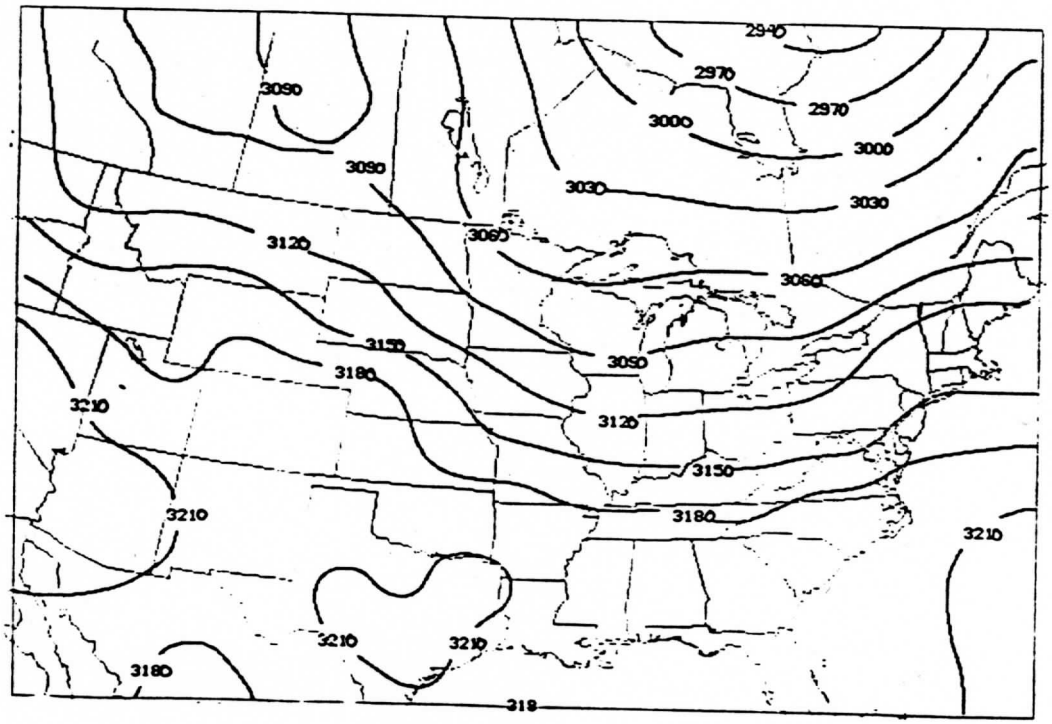

Figure 18a

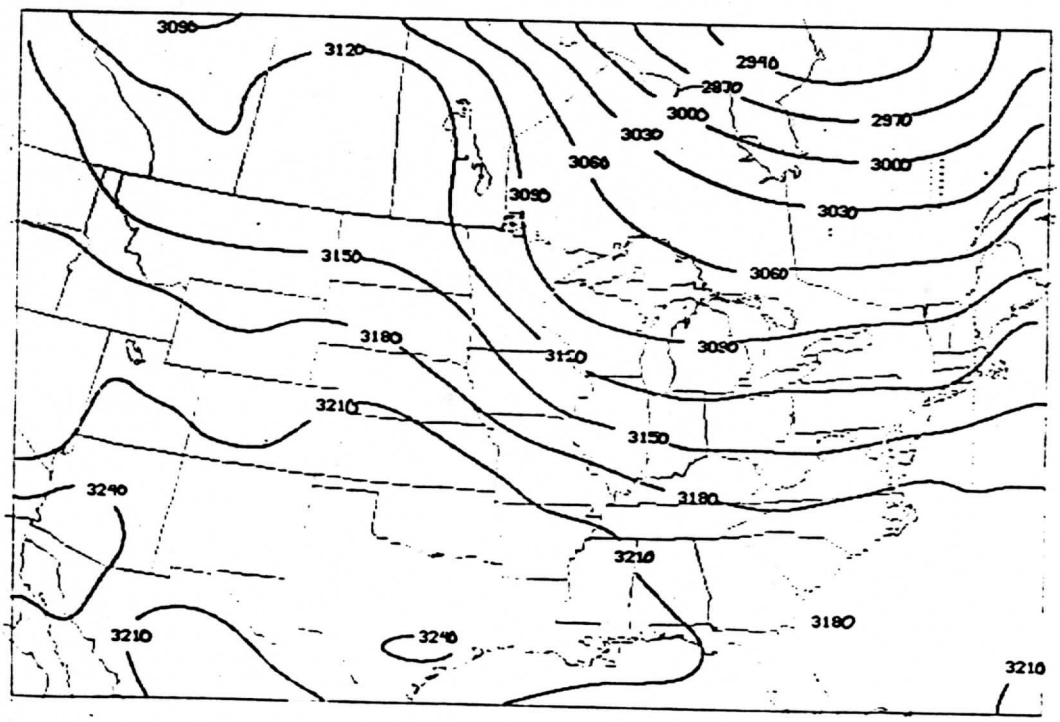

Figure 18b

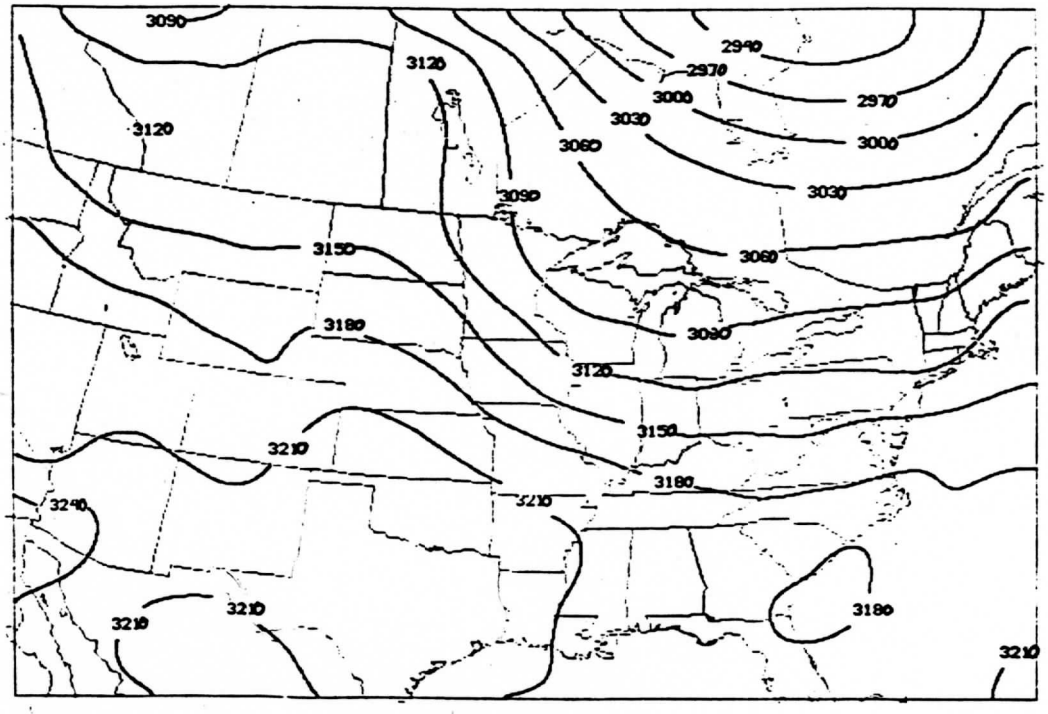

Figure 18c

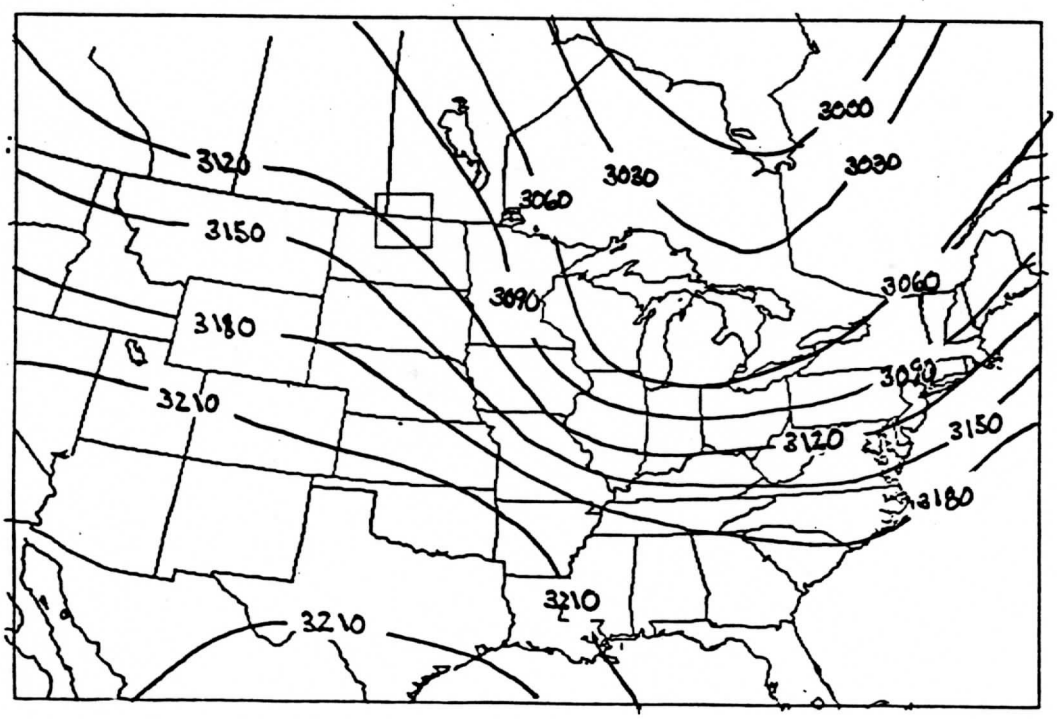

Figure 18d

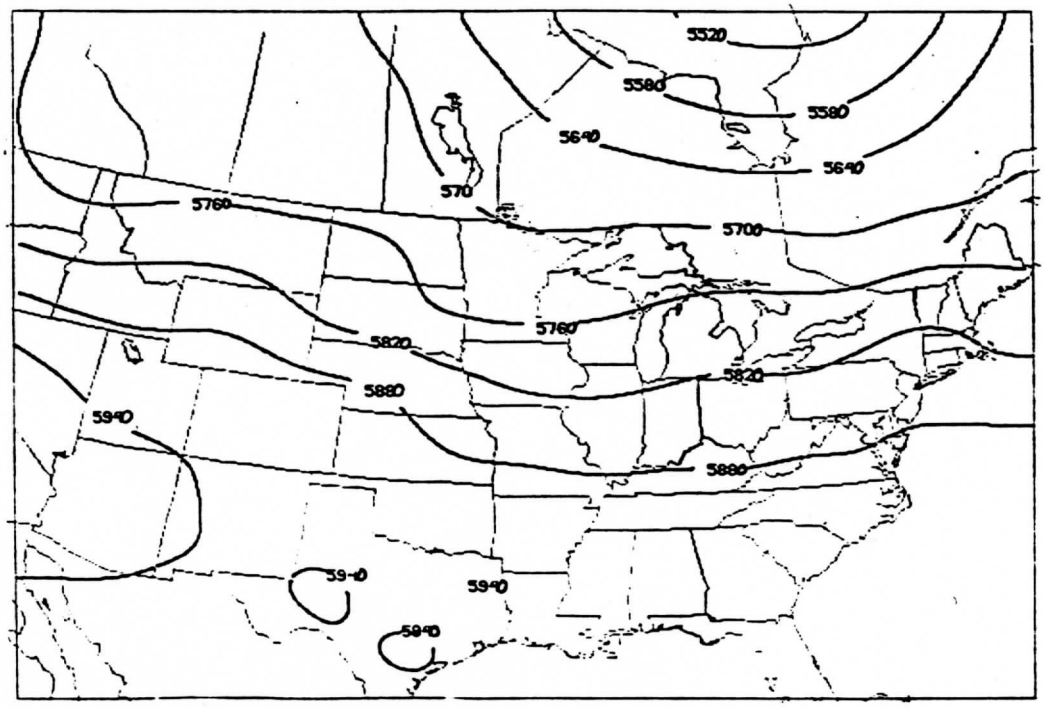

Figure 19a

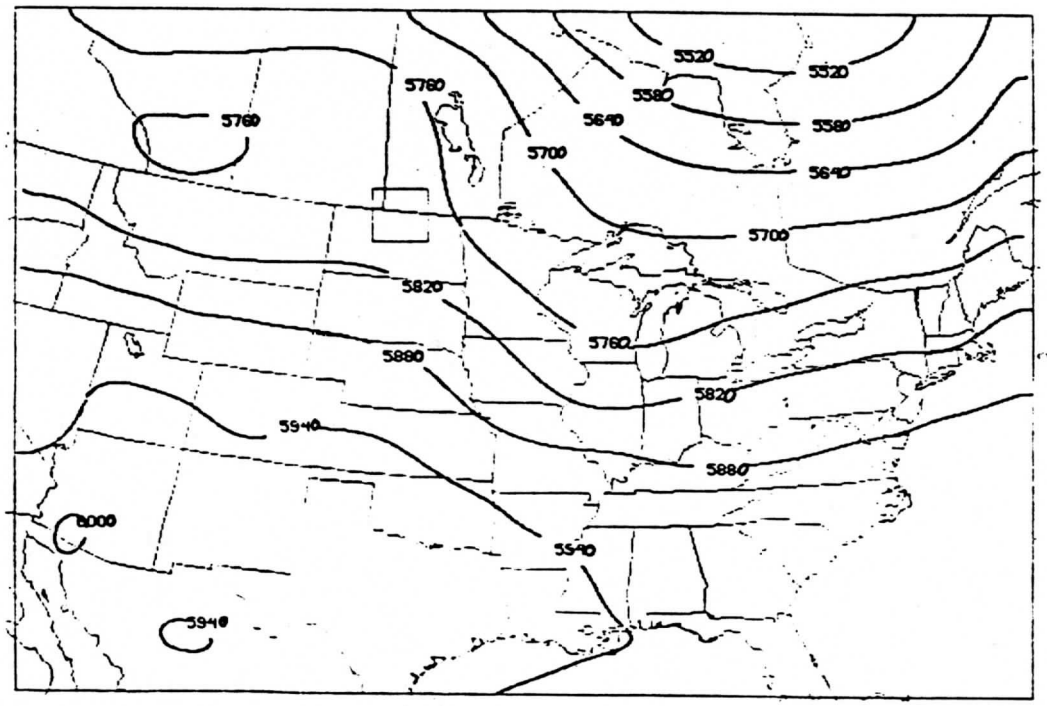

Figuee 19b

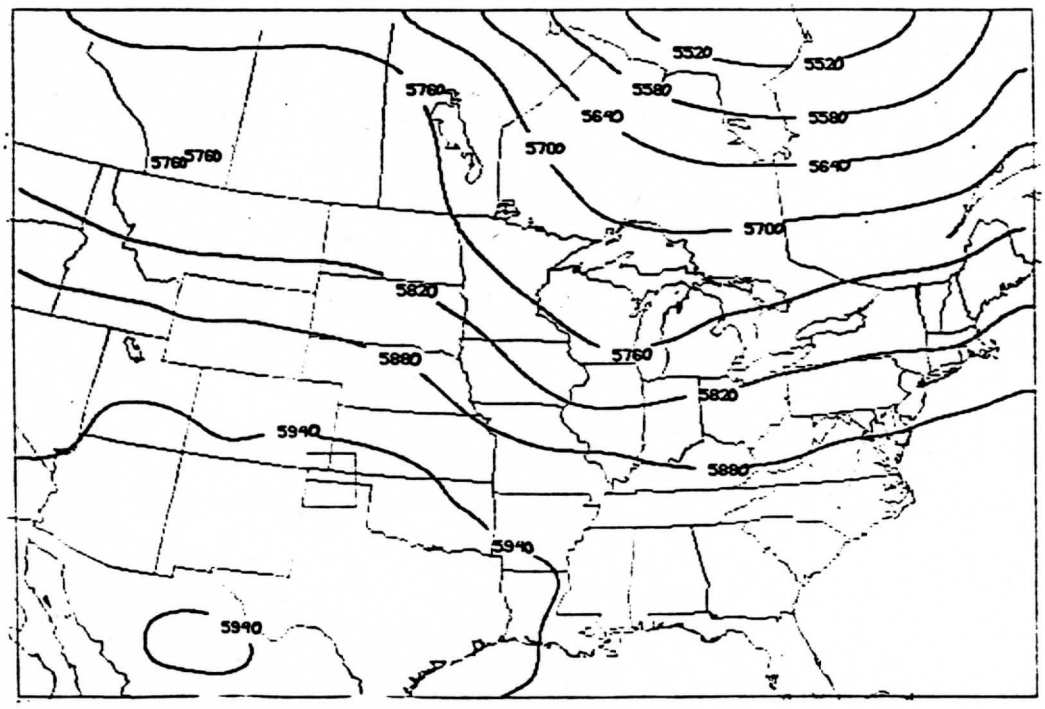

Figure 19c

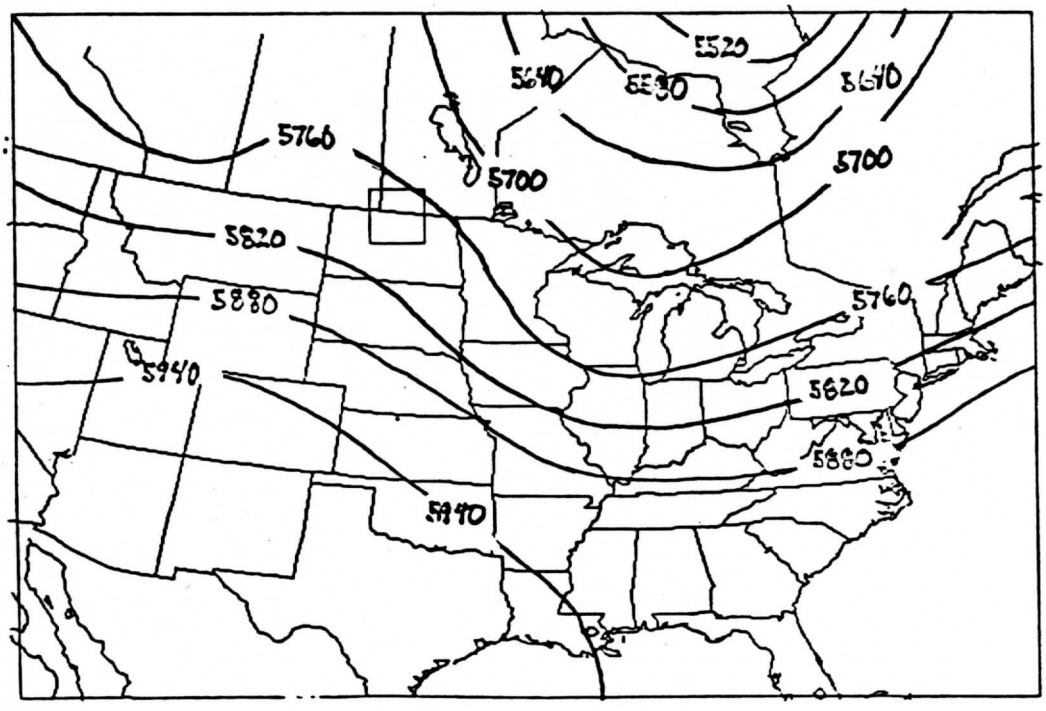

Figure 19d

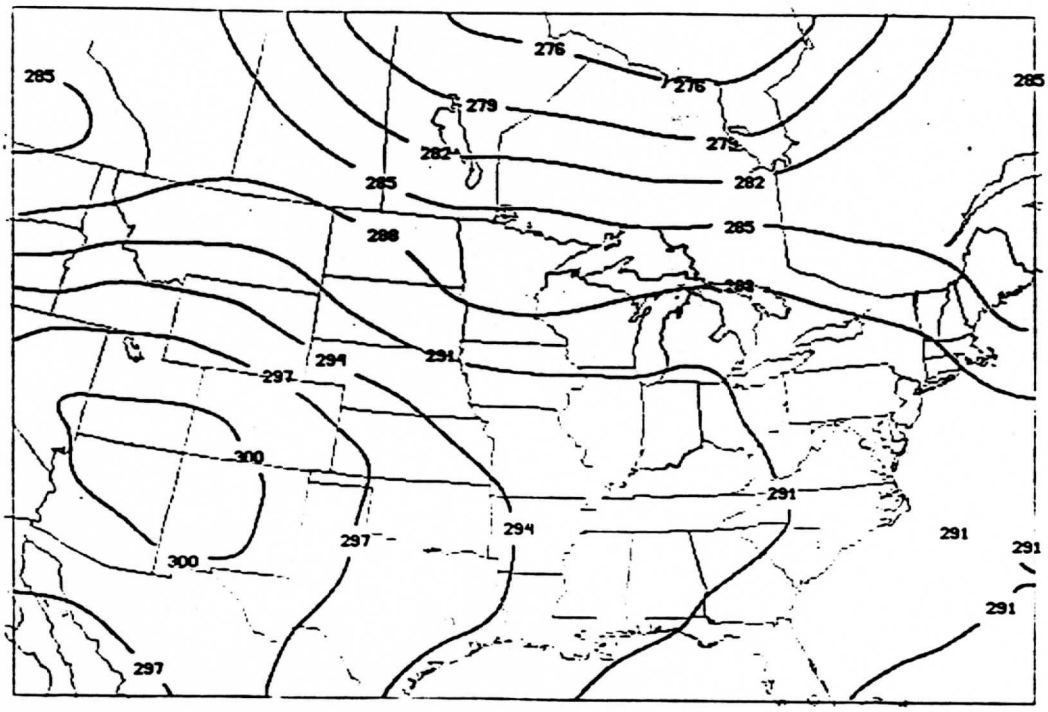

Figure 20a

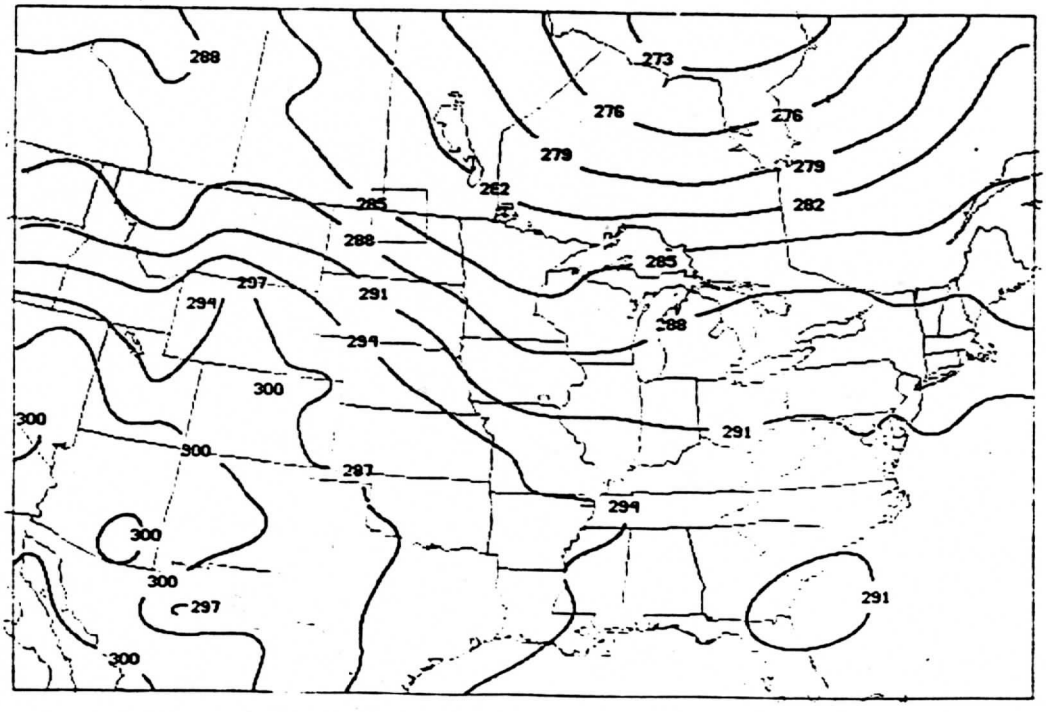

Figure 20b

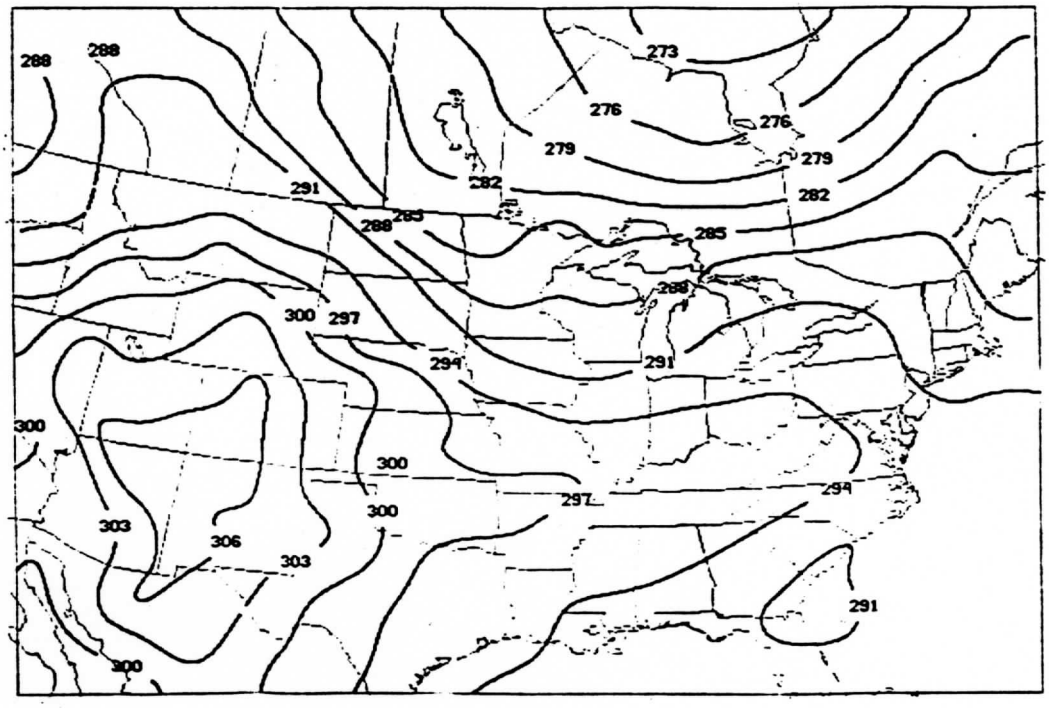

Figure 20c

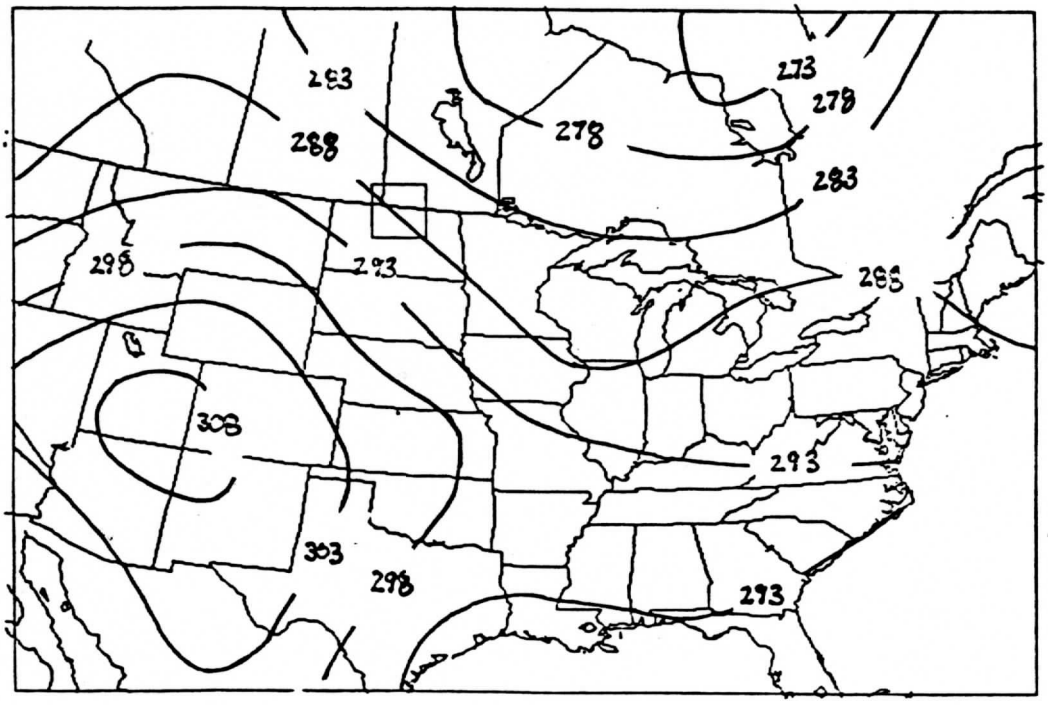

Figure 20d

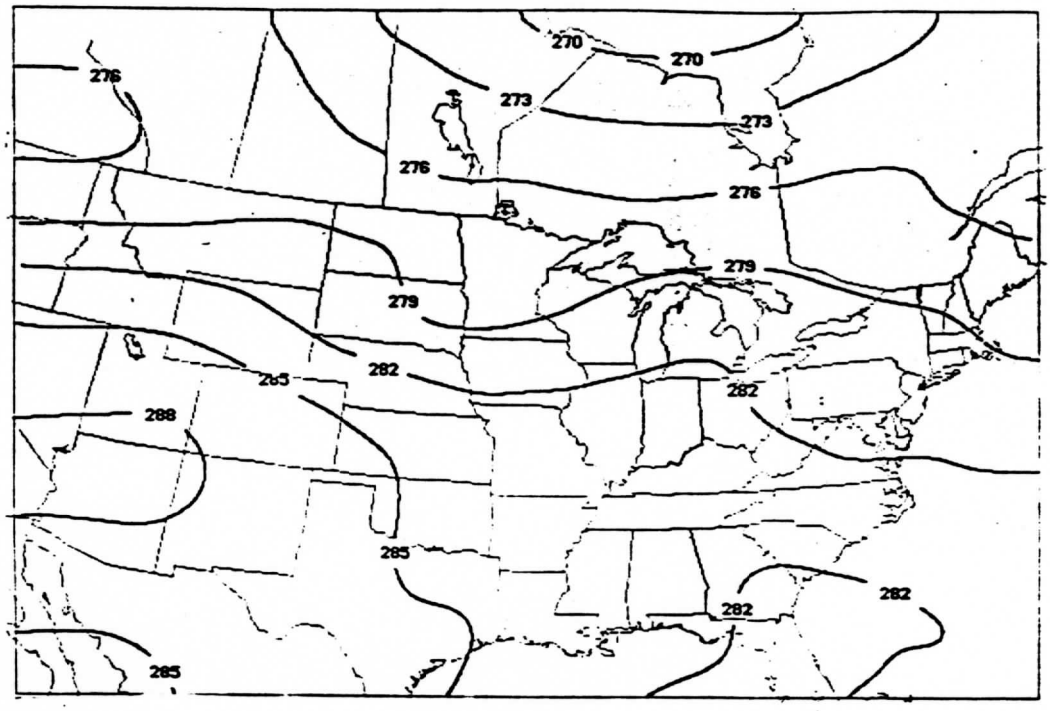

Figure 21a

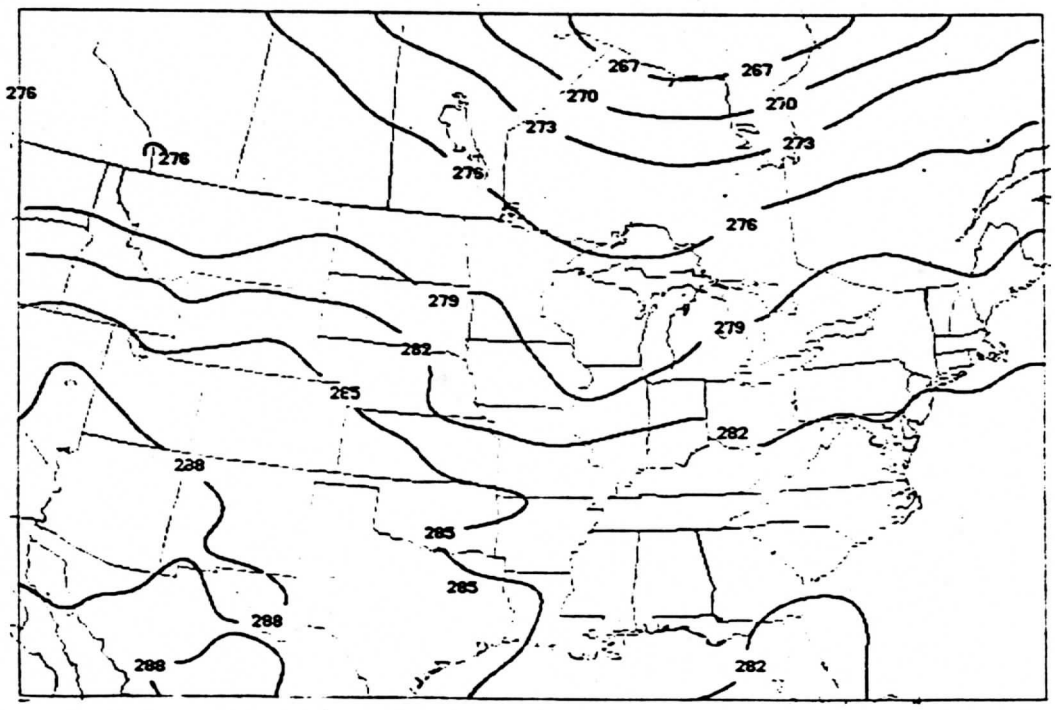

Figure 21b

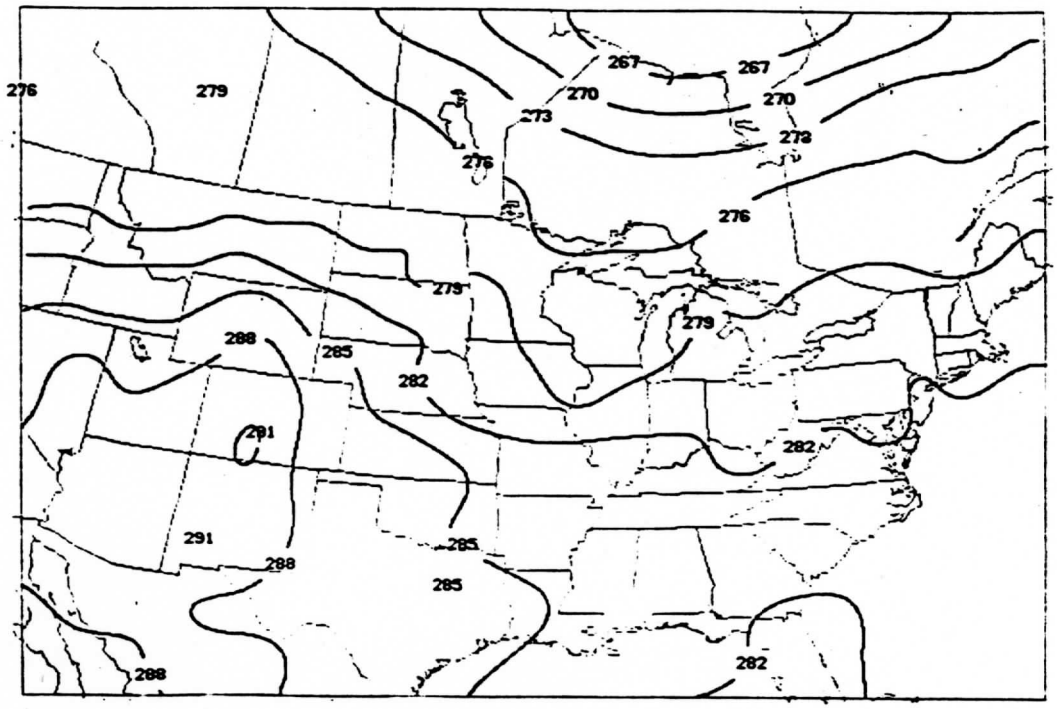

Figure 21c

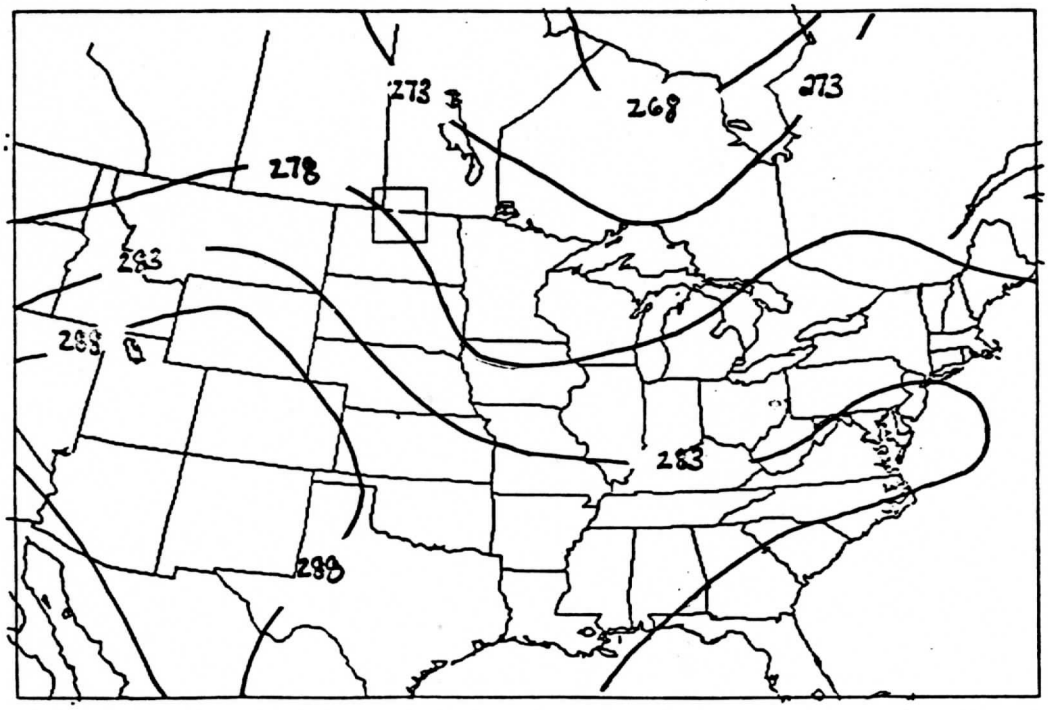

Figure 21d

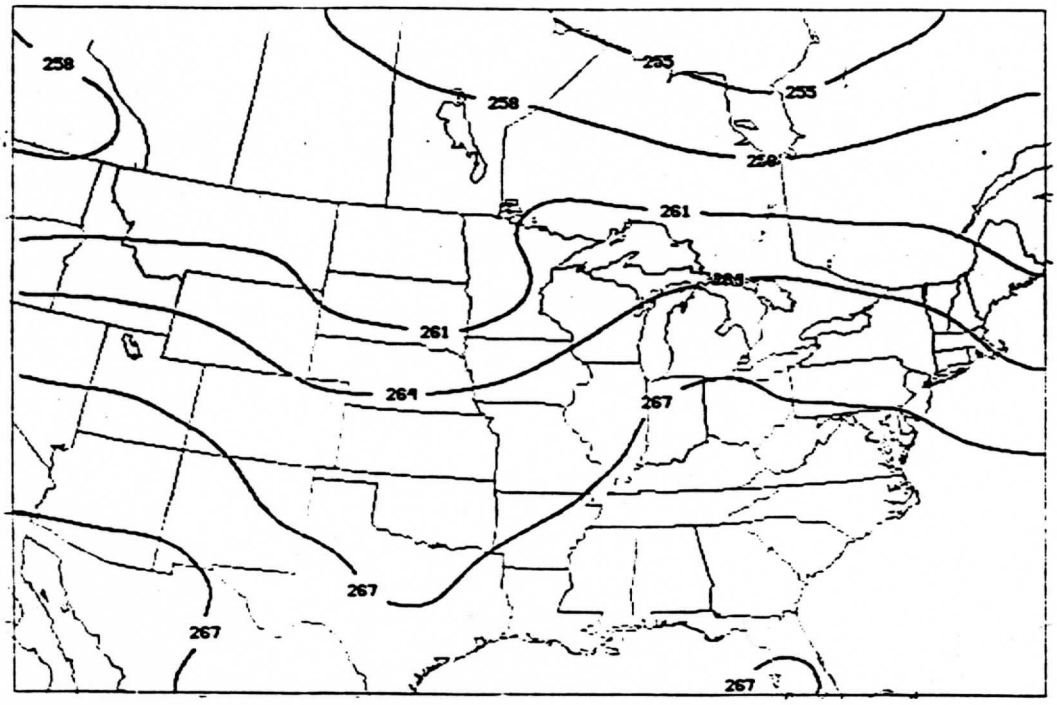

Figure 22a

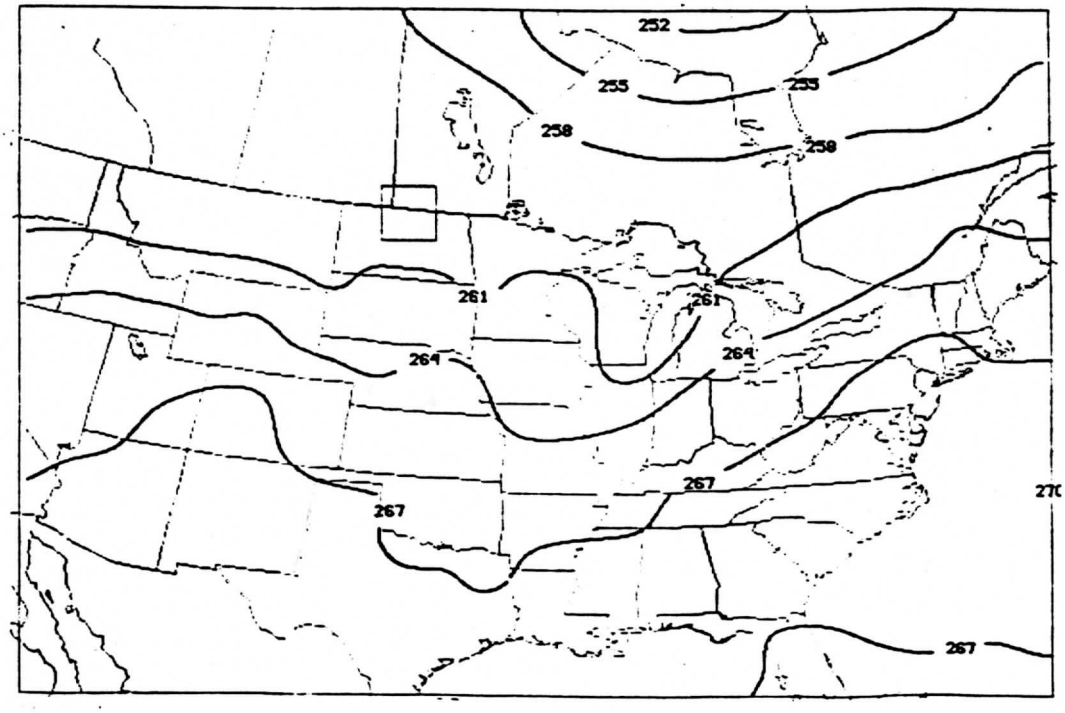

Figure 22b

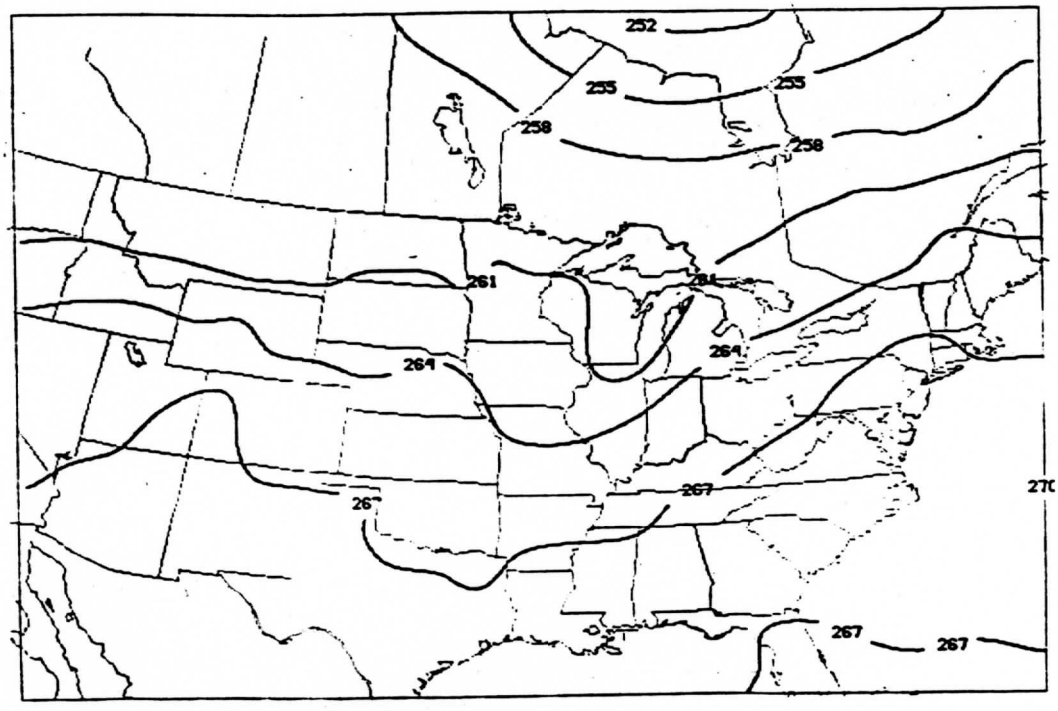

Figure 22c

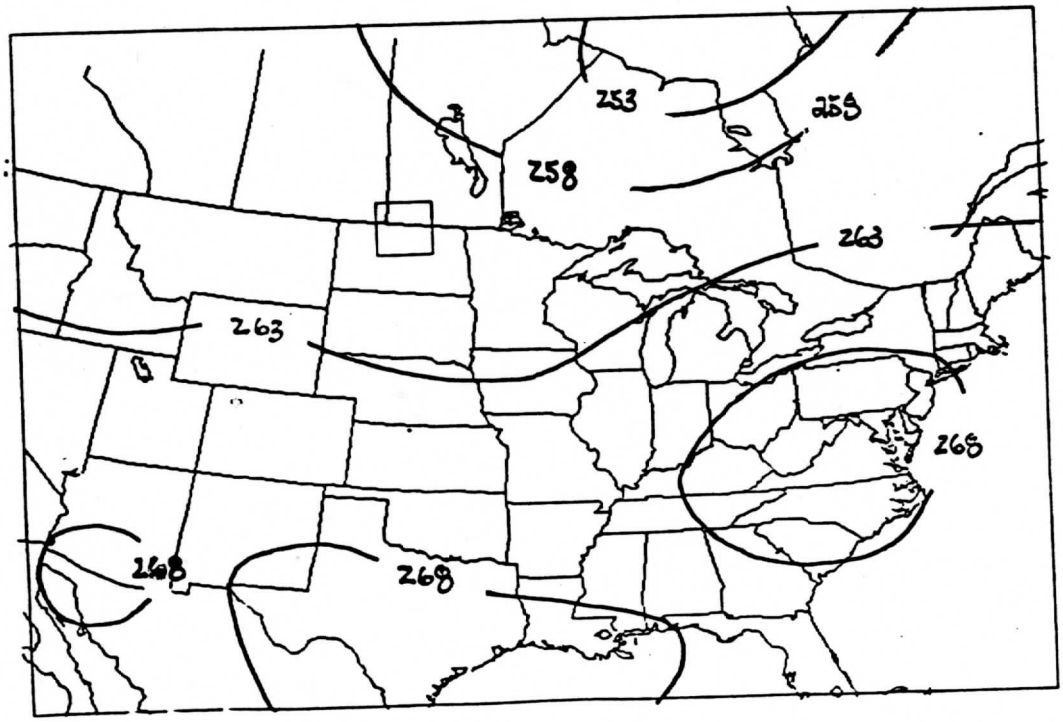

Figure 22d